This is to certify that the
dissertation entitled

FUNCTIONAL ANALYSIS OF CYTOPLASMIC γ-ACTIN MUTATIONS CAUSING NON-SYNDROMIC, PROGRESSIVE AUTOSOMAL DOMINANT HEARING LOSS

presented by

Soumya Korrapati

has been accepted towards fulfillment
of the requirements for the

Doctoral degree in Genetics

Karen Frederici
Major Professor's Signature

21 Oct 2009
Date

FUNCTIONAL ANALYSIS OF CYTOPLASMIC γ-ACTIN MUTATIONS CAUSING NON-SYNDROMIC, PROGRESSIVE AUTOSOMAL DOMINANT HEARING LOSS

By

Soumya Korrapati

A DISSERTATION

Submitted to
Michigan State University
In partial fulfillment of the requirements
for the degree of

DOCTOR OF PHILOSOPHY

Genetics

2009

FUNCTIONAL ANALYSIS OF CYTOPLASMIC γ-ACTIN MUTATIONS CAUSING NON-SYNDROMIC, PROGRESSIVE AUTOSOMAL DOMINANT HEARING LOSS

By

Soumya Korrapati

Mutations in cytoplasmic γ-actin cause non-syndromic, post-lingual, autosomal-dominant, progressive sensorineural hearing loss. LLC-PK1- CL4 cells provide a model system to study the distribution of actins and the role of γ-actin and its mutations in repair of damaged structures like microvilli. Immunohistochemistry and confocal localization studies showed that β-actin was found primarily at the periphery of cells while γ-actin is abundant in the perinuclear space and cytoplasm of the cell. Exogenous expression of mutant γ-actins showed distribution to all the actin structures in the cell; the periphery, stress fibers and perinuclear space. In response to exogenous espin, filamentous mutant actins co-localized with espin in the microvilli. Co-transfection of espin and mutant actin resulted in each of the mutants co-localizing with filamentous actin in the microvilli. Cytochalasin D treatments of WT γ-actin and mutant γ-actins showed no difference in the repair of the damaged microvilli. Measurements of the lengths of microvilli however indicated that the microvilli expressing mutant actins were ~20-25% shorter than the WT γ-actin microvilli. Quantitative FRAP assays heat shock promoter, were used to over-express the mutant actins in the zebrafish. Confocal images of hair cells of cristae and maculae from fish at 4-day post fertilization (dpf) showed that five out of six mutants are expressed in hair

did not reveal any differences in the recovery rates between WT and mutants actins. Our data suggest that mutations in γ-actin exhibit subtle phenotypes and might interfere with basic actin assembly dynamics. To determine the physiological relevance of the cell culture data, a multi-site Gateway system based EGFP tagged WT and mutant γ-actin constructs were made to create a transgenic zebrafish model for the γ-actin mutants. These constructs, under a heat shock promoter, were used to over-express the mutant actins in the zebrafish. Confocal images of hair cells of cristae and maculae from fish at 4-day post fertilization (dpf) showed that five out of six mutants are expressed in hair cells and stereocilia. Fish harboring these mutations did not show any morphological defects and appeared healthy like the WT counterparts.

This dissertation is dedicated to my beloved grandmothers:

Sitaramamma Kurada and Seshamma Korrapati

ACKNOWLEDGMENTS

The credit for the completion of my doctoral degree goes to many wonderful people I have known in my life. I am firstly very grateful to my mentor, Dr. Karen Friderici. She has always shown tremendous faith in my scientific abilities and given me freedom to pursue various avenues during my years as her graduate student. I especially appreciate this trait in her as this has helped me believe in myself. I have learnt a great deal from her. Patience, generosity, honesty and open mindedness are few of the virtues I believe I have inherited from her. She has been a wonderful mentor in every sense. I couldn't have asked for a better scientific advisor.

I am very thankful to my committee members. Dr. Pat Venta, Dr. Steven Heidemann, Dr. David Kohrman and Dr. Laura McCabe for their guidance and insightful suggestions throughout my graduate career. Many thanks to our collaborators Dr. Pete Rubenstein, Dr. Suzanne Thiem and Dr. Jarema Malicki for their guidance and scientific help.

Hard work, sincerity and perseverance are the key to success in life. My parents have always instilled these values in me. They are my support system and have encouraged and supported me all my life in all my endeavors. I am eternally grateful to them for being such wonderful parents. I am also thankful to my brother for his continued love and support. I am lucky to have a sibling who always stands by me and is proud of my achievements. My sincere thanks to my

mother-in-law and father-in-law who have loved me and supported me all along my graduate career.

My heartfelt gratitude to all the lab members of the Friderici lab. They have been wonderful colleagues who made working in the lab a delight. I am especially thankful to Meghan, Ellen, Mei, Kathy and Donna. They all are bright scientists and great friends whom I can always count on. I am very lucky to have found a home in the Friderici lab.

I have met wonderful people during my graduate career and formed lasting friendships. A big thanks to Meghan and Gabe for being great friends. Special thanks to Nitin and Akanksha for their continued love and support. A big thank you to all my friends, (Sireesha, Mukta, Sachin, Amit, Prerna, Lavanya, Kiran, Bhaskar, Priya, Chetan, Rahul, Gauri, Sundari, Sudhakar, Sandhya, Erin, Gabby, Rachel, Rabeah, Tuddow), for being there for me during my graduate career. I greatly appreciate their presence in my life.

Part of the credit for the completion of my PhD goes to my husband and best friend, Tejas. He is my support system. He believed in me more than I believed in myself, never let me give up and always pushed me to become a better scientist. His constant love and support have been instrumental in attaining the degree. I am extremely lucky to have found such a wonderful life partner. Lastly I am thankful to Turbo Taq, my cat for having found me-because he a constant source of joy in my life.

TABLE OF CONTENTS

LIST OF TABLES

LIST OF FIGURES

"Images in this dissertation are presented in color"

LIST OF ABBREVIATIONS

ABM	Actin-bundling module
ACTB	β-actin
ACTG1	γ-actin
ADP	Adenosine di-phosphate
ARHL	Age-related hearing loss
ATP	Adenosine tri-phosphate
Att	Attach sites
BB	Brush border
CD	Cytochalasin D
CMV	Cytomegalovirus
dpf	Days post fertilization
EGFP	Enhanced green fluorescent protein
Ena/VASP	Vasodilator-stimulated phosphoprotein
ENU	N-ethyl N-nitrosourea mutagenesis
ESPN	Espin
EVH1,EVH2	Ena/VASP homology domain1,2
F-actin	Filamentous actin
FRAP	Fluoresence Recovery After Photobleaching
G-actin	Globular actin
hpf	Hours post fertilization
IHC	Inner hair cell

IRES	Internal ribosomal entry site
KO	Knock-out
LLC-PK1-CL4	Pig proximal kidney epithelial clone 4 cells
OHC	Outer hair cell
PFA	Para formaldehyde
pDest	Destination vector
pDONR	Donor plasmid
PR	Proline rich
SEM	Scanning elctron microscopy
siRNA	Small interference RNA
SNHL	Sensorineural hearing loss
UTR	Untranslated region
WASP	Wiskott-aldrich syndrome protein
WH2	Wiskott-aldrich syndrome protein homology domain
WT	Wild type

CHAPTER 1

Literature Review

Introduction

The goal of my research is to evaluate how cytoplasmic γ-actin mutations cause autosomal dominant, non-syndromic, late-onset progressive hearing loss. The approach I use relies primarily on a cell culture model but I have also explored a zebrafish model to examine the effect of mutations in γ-actin. To evaluate the appropriateness of these models, I will provide a brief review of the mammalian ear, cell biology and physiology of inner ear, the process of hearing and the genetics of hearing loss.

1 Anatomy of the ear

The mammalian ear is compartmentalized into outer ear, middle ear and inner ear (Figure 1-1). Mechanical stimulus is converted into electrical signal by the orchestrated activity of these three compartments. The outer ear is made up of an auricle or pinna and a 2 cm auditory canal [1]. The primary function of the pinna is to concentrate and direct the sound waves into the auditory canal. It also serves as a shield to protect the middle ear structures from damage. Sound waves, which are in the form of pressure waves, are collected by the ear canal and channelized to the middle ear. A stretched membrane known as the eardrum or tympanic membrane, and three interconnected ossicles-incus, malleus and stapes, constitute the middle ear [1]. The pressure waves from the ear canal are received by the tympanic membrane causing it to vibrate. These vibrations set the ossicles in motion, which amplify the sound waves. These waves are then transmitted to the inner ear via the stapes. The cochlea in the inner ear is

responsible for converting the sound waves into an electrical signal while the vestibule maintains a sense of gravity, acceleration and balance. Both cochlea and the vestibule send the electrical signal to the brain via the auditory nerve. In the following section I will describe the inner ear components in detail.

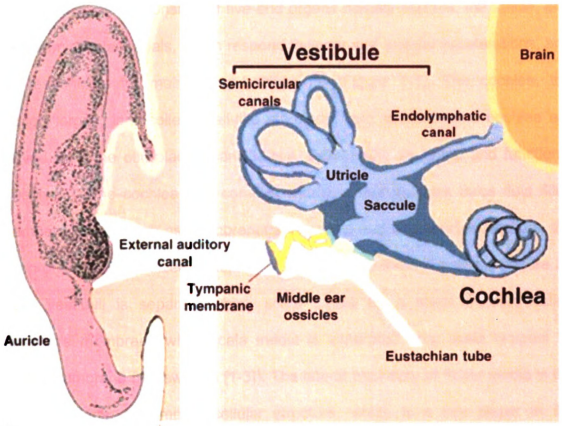

Figure 1-1: Schematic representation of the human ear. It is divided into outer, middle and inner ear. Auricle and auditory canal constitute the outer ear, while the tympanic membrane and the three middle ear ossicles (incus, malleus and stapes) form the middle ear. The vestibule and the cochlea constitute the inner ear. Semicircular canals, utricle, saccule and the endolymphatic canal form the vestibular system while organ of Corti and membranous labyrinth constitute the cochlea (modified from [1]).

2 Inner Ear and Hearing

2.1 Inner ear physiology

The vestibule consists of five-end organs namely saccule, the utricle, and three semicircular canals, which respond to linear and angular accelerations, and are responsible for maintaining balance [1] (Figure 1-1). The cochlea, the auditory organ, is a coiled snail-like structure. Both vestibule and cochlea are derived from the otic placode and hence share many structural and functional aspects [1]. The cochlea is a complex structure that includes three fluid filled chambers (also known as membranous labyrinth) and a sensory epithelium, the organ of Corti. Specialized structures separate these three chambers (Figure 2). Scala vestibuli is separated from scala media by a sheet of cells called Reissner's membrane while scala media is separated from scala tympani by basilar membrane (reviewed in [1-3]). The lateral boundary of Scala media is the stria vascularis, a complex cellular structure, which is a key player in the generation of endocochlear potential and is home to many Na-K-ATPases, which play a critical role in K^+ recycling [4] (Figure 1-2). Scala vestibuli and scala tympani are actually contiguous and are filled with perilymph, while scala media is filled with endolymph. A cross-section through a turn of the snail shaped cochlea shows that the apical side of the organ of Corti is bathed in the endolymph while the baso-lateral side is in the perilymph (reviewed in [1-3]) (Figure 1-2).

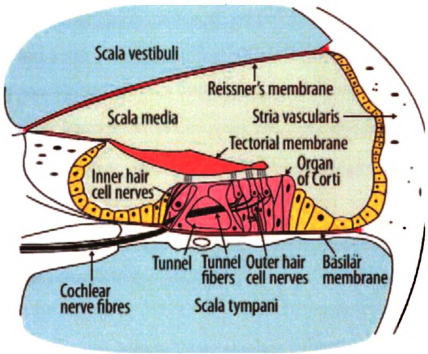

Figure 1-2: Schematic of the cross-section of inner ear. It consists of three fluid filled compartments namely scala vestibuli, scala media and scala tympani. Scala vestibuli and scala media are separated by Reissner's membrane, while the basilar membrane separates scala media and scala tympani. Scala media on one end is lined by stria vascularis. Organ of Corti consists of inner and outer hair cells and non-sensory supporting cells and rests on the basilar membrane. Tectorial membrane lies on the hair cells, contacting a subset of the stereociliary bundles (modified from [5]).

Perilymph and endolymph differ from each other in their ion concentrations. Where perilymph is high in Na^+ (140mM) and low in K^+ (3.5mM), endolymph has a rare composition of very high K^+ (about 150mM) and very low Na^+ (1mM) (reviewed in [1, 3, 4]). The difference in ion concentrations results in an endocochlear potential of +80 mV, believed to be the largest in the body [2]. There are advantages to having K^+ as the major charge carrier for sensory transduction in the inner ear. K^+ being the most abundant ion in the cytosol, influx of K^+ results in the least change in the cytosol and, influx and extrusion of K^+ ions are energetically inexpensive to the cell [4].

Various cell types like the ion-transporting epithelia, sensory epithelia, and relatively unspecialized epithelia add an additional layer of complexity to the cochlear structure [6, 7]. The ion-transporting epithelia are the stria vascularis and regions of the vestibular system, which as mentioned earlier play an active role in recycling the K^+ ions to maintain the endolymph composition. Reissner's membrane and the roofs of the semicircular canals form the unspecialized epithelia, which help in separating the two fluid compartments [3]. Organ of Corti is the sensory epithelium of the cochlea while the vestibular system consists of five sensory epithelial sheets, namely the maculae of the utricle and saccule and the three cristae, one in each semi-circular canal [3]. The sensory epithelia are composed of sensory hair cells and supporting cells. Various supporting cells like pillar cells, Deiters cells, and cells of Hensen, provide support to and help

maintain the hair cells. They surround the hair cells such that no two hair cells are in contact with each other [6] (Figure 1-3A). Tight junctions seal the apical boundaries of hair cells and surrounding supporting cells [1]. The supporting cells are inter-connected by gap junction proteins, which play a critical role in the homeostasis of the cochlear fluids [6]. Gap junctions are sites of direct communication between adjacent cells via continuous aqueous hemichannel pores known as connexons. These pores allow the passage of small metabolites (glucose, ATP,~1200Da), messengers (cAMP, inositol 1,4,5 triphosphate-IP3) and ions thereby acting as sites of electrical and chemical coupling [3]. Connexin (Cx) protein family members form the hemichannel pore or connexon. Five of the twenty-one connexin isoforms are expressed in the mammalian cochlea [8]. Of these, mutations in the Cx 26 isoform account for 50% of non-syndromic autosomal recessive hearing loss [8].

2.2 Sensory hair cells

In the organ of Corti, inner hair cells (IHCs) and outer hair cells (OHCs) are the two kinds of sensory hair cells, while type 1 and type 2 are the sensory hair cells found in the vestibular system (reviewed in [1, 3]). These two kinds of hair cells show unique innervation patterns. In the organ of Corti, IHCs are innervated exclusively with afferent nerves and are considered the true sensory cells, as they send the impulses to the brain via the afferent auditory nerve [7]. OHCs, on the other hand, act as amplifiers of the auditory signal and are innervated with efferent nerves [7]. The sensory hair cells are overlaid by an

extracellular matrix known as tectorial membrane in cochlea, otolithic membranes in macular organs and cupulae in cristae [3].On the bottom, the sensory epithelia rest on a basement membrane known as basilar membrane (Figure 1-2).

IHCs are pear shaped cells with centrally located nucleus [3] (Figure 1-3A). A single row of IHCs runs along the cochlear duct. OHCs are cylindrical in shape with the nucleus at the bottom of the cylinder [3, 7] (Figure 1-3A). Three rows of OHCs are present in the organ of Corti, but in some mammals a fourth or fifth row has also been observed [7]. Each hair cell has 30-300 apical projections on its surface, known as stereocilia [1, 3, 7, 9-11]. The stereocilia on the IHCs are arranged in a W shaped pattern, while those on OHCs have a V shaped arrangement [3] (Figure 3B). Unlike true ciliary structures, stereocilia are in fact, derivatives of actin-based microvilli [1, 3, 7, 9-11].

Because γ-actin plays a central role in maintaining cellular structure, it is conceivable that any of the cells described so far could be adversely affected by mutations in this protein. However, the pivotal role of stereocilia in hearing and the exceptional enrichment of cytoplasmic actin in these structures make them attractive targets for study of the potential affect of the mutations in γ-actin. Therefore the following sections are especially pertinent to my thesis work.

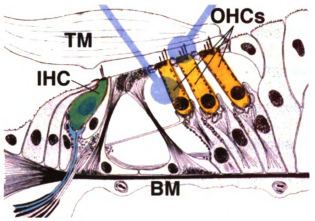

Figure 1-3A: Cross section of organ of Corti. There are three rows of outer hair cells that are cylindrical in shape and the nucleus is towards the bottom of the cell body. On the other hand, inner hair cells are pear-shaped and the nucleus is the center of the cell body. IHC: inner hair cell, OHCs: outer hair cells, TM: tectorial membrane, BM: basilar membrane (modified from [12]).

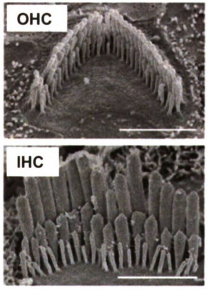

Figure 1-3B: Scanning electron microscopy images of OHC and IHC. Stereocilia on outer hair cells are arranged in a V shape and those on inner hair cells have a W shaped pattern (modified from[13]).

2.3 Stereocilia

Stereocilia are arranged in precisely specified rows of increasing heights forming a characteristic staircase-like structure on the surface of the cell [1, 3, 7, 9-11] (Figure 1-4). The longer stereocilia of all hair cells are in contact with the tectorial membrane [3]. The arrangement of stereocilia on the hair cells is tightly regulated; length and width, position and orientation are all critical to proper hearing. The position of the stereocilia is determined by the true cilium, the kinocilium. Stereocilia development is well studied in the avian auditory hair cells and mammalian vestibular hair cells [10, 14]. Barring a few inter-species and inter-organ differences, the overall features of stereocilia development are as follows. A single kinocilium appears on the surface of the hair cell, surrounded by numerous precursor microvillus projections. The microvilli then stop elongating and widen instead. Eventually the kinocilium migrates to the edge of the cell surface, thus determining the polarity of the stereociliary bundle. The microvilli then elongate sequentially to form the staircase–like bundle, where the longest stereocilia is next to the kinocilium. The stereociliary rootlets project into the cuticular plates to anchor the stereocilia. The microvilli that fail to become part of the staircase regress into the cell. The kinocilium in the cochlear hair cells also regresses into the cell and is reduced to a basal body. Thus the auditory hair cell gains the stereociliary staircase structure (Figure 1-4) and is devoid of the kinocilium. In addition to detecting sound amplitude, hair cells also detect sound frequencies based on their position. Interestingly, the frequencies are distributed across the stereocilia such that higher frequencies are detected by stereocilia on

the basal turn of the cochlea while lower frequencies are detected by the stereocilia on the apical turn. Thus the stereociliary structure, along with the lengths, numbers and bundle shape are important for the sensitivity of the hair cell. Tilney & Tilney very accurately note in their paper that the hair cell in the cochlea "is perhaps the most extraordinary example of precision engineering seen anywhere in the vertebrate organism [10]".

Individual stereocilia are held together at various points along their entire length such that they are deflected together, in response to sound waves [1, 3]. They are held together by ankle links at the base, by side links along the sides and by tip links at the top (Figure 1-5) [1, 7, 11, 15, 16].

Figure 1-4: Stereocilia bundle. The stereocilia form a staircase-like structure consisting of increasing heights of individual stereocilia. The tallest of the stereocilia lies next to the kinocilium-which decides the polarity of the bundle. The bundle is held together at different locations along the entire length (modified from [15]).

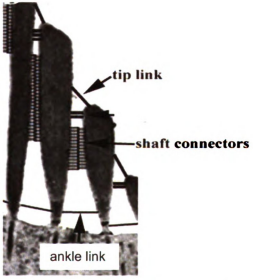

Figure 1-5: Various interstereociliary cross-links. Tip links connect the top of a short stereocilium and shaft of the adjacent taller stereocilium. Tip links contain the gated ion channels. Shaft connectors connect shafts of adjacent strereocilia and the ankle links connect adjacent stereociliary ankles. Modified from [3].

2.4 Hearing

In response to stimuli/vibrations from the middle ear, the basilar and tectorial membranes are set in motion. This motion causes the stereocilia to deflect as a whole, towards the longest stereocilia (Figure 1-6). This deflection creates tension at the tip links, which are filaments that connect the apical surface of the shorter stereocilium to the lateral wall of the adjacent taller stereocilium [1]. This tension causes the gated channels to open letting the K^+ ions from the endolymph into the hair cells, causing them to depolarize. The voltage channels open and Ca^{2+} ions enter the cell. This triggers the release of neurotransmitter onto the afferent fibers. The nerves then transmit the electrical signal to the brain. Recycling of K^+ ions occurs basolaterally from hair cells and via the gap junctions of the supporting cells. The gated channels close, the cells recover their resting potential and the stereocilia regain their shape [3].

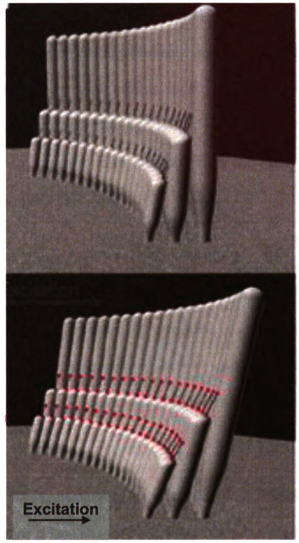

Figure 1-6: Schematic of stereocilia deflection. Sound-induced excitation results in nanometer-scale deflections of the hair bundle towards the longest stereocilia. This opens mechanically gated ion channels (shown in red)(modified from [16]).

3 Hearing Loss

3.1 Characterization of hearing loss

Humans hear in the range of 20-20,000 hertz and 28-35 million Americans suffer from a hearing impairment, that affects their quality of life [1, 17, 18]. Seventeen out of 1000 children under the age of 18, and 34 out of 1000 people by the age of 65 suffer from hearing loss, the statistics increase to 40-50% in individuals over 75 (NIDCD, [17, 19]).

Hearing loss can be divided into various categories. It is classified into mild (20-40dB), moderate (40-60dB), severe (60-80dB) or profound (80 and more) based on the loudness required to produce a response at various frequencies [20]. Hearing loss due to mutations in the γ-actin gene begins as mild loss at high frequencies which progresses to profound loss with advancing age [21, 22].

Hearing loss can be conductive, sensorineural or mixed. Conductive hearing loss relates to hearing impairment resulting from the malfunction of the outer or middle ear structures. Tympanic membrane perforation, ossicular discontinuity or fixation, earwax build-up, otitis externa and otitis media (external ear and middle ear infections, respectively) or reactions to certain drugs like chloroquine, may result in conductive hearing loss [23]. This kind of hearing loss is reversible following wax clean up or treatment of the infections [23]. Sensorineural hearing loss (SNHL) results from the pathologies of the inner ear and the auditory nerve. It is believed to be the cause of 70% of all hearing loss

[24]. SNHL can result from aging, noise exposure, toxic drug exposure, viral infections (rubella virus-from mother to fetus), and genetic factors. Hair cells of the mammalian organ of Corti are terminally differentiated and they do not regenerate following damage [2]. Hence SNHL is a permanent condition and there is no cure/treatment. Hearing loss occurring from the malfunction of outer or middle ear along with inner ear or auditory nerve is known as mixed hearing loss. All γ-actin mutations described to date cause SNHL.

Hearing loss is often accompanied as a phenotype in many human syndromes. Over 400 syndromes with hearing loss have been described [25]. Syndromic hearing loss accounts for 30% of all cases of hearing loss [1]. Non-syndromic hearing loss occurs due to environmental factors and/or genetic factors. The hereditary forms of non-syndromic hearing loss can be Y-linked, X-linked, autosomal dominant, autosomal recessive and mitochondrial DNA (mtDNA) linked [20]. Mutations in the γ-actin gene cause autosomal dominant, non-syndromic, late onset hearing loss [21, 22].

3.2 Age related hearing loss (ARHL) or Presbycusis

ARHL affects the quality of life of adults, a condition that is a polygenic and/or multifactorial in nature [18]. It results in bilateral hearing loss and is the most common cause of hearing loss in adults [26]. ARHL starts initially as high frequency hearing loss that has adverse affects on communication. ARHL is believed to be a result of age dependent atrophy of cochlea and age related

accumulation of noise insults [18]. Based on the region of cochlea that degenerates, ARHL can be sensory, neural, strial or metabolic [18, 26]. Degeneration of the lateral wall of stria vascularis is believed to be one of the contributors to ARHL [18]. Audiograms of such persons show hearing loss across all frequencies, thereby exhibiting a flat loss [26]. This view is supported by evidence of age-related loss of expression of Na-K-ATPases in the stria vascularis, followed by dramatic loss of the endocochlear potential [18]. Sensory presbycusis is the most common type of ARHL in adults, whose cochlear pathologies and audiograms are very similar to those of non-syndromic late-onset hearing loss individuals [18].

Though a significant portion of AHRL (~40-50%) is genetically determined, the molecular etiology of presbycusis still remains unknown [22]. Barring the age of onset, phenotype and progression of AHRL and late-onset hearing loss are similar. Hence, genes involved in non-syndromic late-onset hearing loss might be excellent candidates to study the pathophysiology of ARHL. γ-Actin mutations, we believe is one such promising candidate.

All the γ-actin mutations identified so far result in hearing loss, like in presbycusis, initially in high frequencies. With age the hearing loss becomes progressive and extends into all frequencies [21, 22, 27-29]. Besides shedding light on the role of γ-actin in hair cells, research on these mutations might provide us with clues about the molecular pathology of ARHL.

3.3 Genetics of hearing loss

The role of genetics has been well established in the pathogenesis of hearing loss. Nearly 130 genetic loci have been identified as the cause of non-syndromic hearing loss, while many of the underlying genes still remain to be determined [19, 25]. Mouse models have been pivotal in dissecting the genetics and pathophysiology of hearing loss [19, 30]. Almost identical ear architecture and physiology between mice and humans, the close genetic relationship (~99% of mice genes have a human orthologue) and the occurrence of spontaneous deaf mice have been invaluable to researchers in unveiling the genetic components of the hearing process [19]. In addition, phenotype-oriented and gene-oriented mutagenesis screens have been other clever techniques used to delineate the various gene products involved in hearing [19]. SNHL can occur due to mutations in genes expressed in any region of the inner ear. A list of proteins expressed in different cell types of the inner ear, mutations in which cause either sensory or vestibular defects in humans and mice, is shown in Table 1 [20]. The best known and most studied are the connexin family members of which *GJB2*, coding for connexin 26 protein, is responsible for causing the most prevalent genetic form of autosomal recessive hearing loss [8]. It is evident from these examples that the inner ear is a very specialized and complex structure, which houses a myriad of proteins. It is also true that most of these proteins are not ear-specific yet the expression of these genes is critical for normal functioning of this structure.

I am particularly interested in the bundling protein espin and the mutations in the actin gene because two of the six initially identified actin mutations are in a predicted protein-binding domain of actin. In addition, one of those (T89I) is identical to a yeast actin mutation found in a complementation screen for an actin-bundling protein [31]. In the following sections, I will describe the role and function of actin and espin proteins in the hair cells and hearing.

Table 1-1. Genes underlying isolated deafness as a result of primary defects in hair cells, non-sensory cells and the tectorial membrane or unknown cell type and corresponding mouse mutants (modified from [20]).

Primary defect	Gene	Gene product	Forms of human deafness	Mouse mutants
Hair cells	*MYO7A*	Myosin VIIA (motor protein)	DFNB2±retinopathy (Usher 1B) DFNA11	Shaker-1 (*Sh1*)
	MYO15	Myosin XV (motor protein)	DFNB3	Shaker-2 (*Sh2*)
	MO6	Myosin VI (motor protein)	DFNA22±cardiomyopathy	Snell's waltzer (*Sv*)
			DFNB37	
	MYO3A	Myosin IIIA (motor protein)	DFNB30	
	MYO1A	Myosin IA (motor protein)	DFNA48	
	ACTG1	γ-Actin (cytoskeletal protein)	DFNA20 (DFNA26)	
	USH1C	Harmonin (PDZ domain-containing protein)	DFNB18±retinopathy (Usher 1C)	Deaf circler (*Dfcr*)
				Deaf circler 2 Jackson (*Dfcr-2J*)
	WHRN	Whirlin (PDZ domain-containing protein)	DFNB31	Whirler (*Wi*)
	CDH23	3 (cell-adhesion protein)	DFNB12±retinopathy (Usher 1D)	Waltzer (*V*)

Table 1-1 contd

Primary defect	Gene	Gene product	Forms of human deafness	Mouse mutants
	PCDH15	Protocadherin-15 cell-adhesion protein)	DFNB23±retinopathy (Usher 1F)	Ames waltzer (*Av*)
	TMIE	TMIE (transmembrane domain-containing protein)	DFNB6	Spinner (*Sr*)
	STRC	Stereocilin	DFNB16	
	SLC26A5	Prestin (anion transporter)	DFNB61	*Slc26a5*
	ESPN	Espin (actin-bundling protein)	DFNB36, $DFNA_i$	Jerker (*Je*)
	KCNQ4	KCNQ4 (K^+ channel subunit)	DFNA2	
	TMC1	TMC1 (transmembrane channel-like protein)	DFNB7 (DFNB11), DFNA36	Deafnes s (*Dn*) Beethov en (*Bth*)
	OTOF	Otoferlin (putative vesicle traffic protein)	DFNB9	
	POU4F3	POU4F3 (transcription factor)	DFNA15	*Brn3c* Dreidl (*Ddl*)
Non-sensory cells	*GJB2*	Connexin-26 (gap junction protein)	DFNB1, DFNA3±keratodermia (Vohwinkel, palmoplantar keratoderma, KID, Bart-Pumphrey)	*Cx26*
	GJB6	Connexin-30 (gap junction protein)	DFNB1, DFNA3±keratodermia (KID)	*Cx30*
				$Cx26^{+/-}$/ *Cx30*

Table 1-1 contd

Primary defect	Gene	Gene product	Forms of human deafness	Mouse mutants
	GJB3	Connexin-31 (gap junction protein)	DFNA	
	SLC26A4	Pendrin (I^-–Cl^- transporter)	DFNB4±thyroid goiter (Pendred)	*Pds*$^{-/-}$
	CRYM	μ-Cristallin (thyroid hormone-binding protein?)	DFNA	
	OTOA	Otoancorin (cell-surface protein)	DFNB22	
	CLDN14	Claudin-14 (tight-junction protein)	DFNB29	*Cldn14*$^{-/-}$
	COCH	Cochlin (extracellular matrix component)	DFNA9	
	TMPRSS3	TMPRSS3 (transmembrane serine protease)	DFNB8 (DFNB10)	
	MYH9	Myosin IIA (motor protein)	DFNA17±giant platelets (Fechtner)	
	MYH14	Myosin IIC (motor protein)	DFNA4	
	EYA4	EYA4 (transcriptional coactivator)	DFNA10	
	POU3F4	POU3F4 (transcription factor)	DFN3	fidget (*slf*)
				Brn4$^{-/-}$

Table 1-1 contd

Primary defect	Gene	Gene product	Forms of human deafness	Mouse mutants
Tectorial membrane	*COL11A2*	Collagen XI (α2-chain) (extracellular matrix component)	DFNA13±osteochondro-dysplasia (Stickler 2)	*Col11a2* $^{-/-}$
	TECTA	α-Tectorin (extracellular matrix component)	DFNA8 (DFNA12), DFNB21	*Tecta* $^{-/-}$
Unknown	*HDIA1*	Diaphanous-1 (cytoskeleton regulatory protein)	DFNA1	
	DFNA5	Unidentified	DFNA5	*Dfna5* $^{-/-}$
	WFS1	Wolframin (endoplasmic-reticulum membrane protein)	DFNA6 (DFNA14, DFNA38)±diabetes and optic atrophy (Wolfram)	
	TFCP2L3	TFCP2L3 (transcription factor)	DFNA28	
	MTRNR1	Mitochondrial 12S rRNA	ND	
	MTTS1	Mitochondrial $tRNA^{ser(UCN)}$	ND	

Abbreviation: ND, not defined nomenclature.

4 Actin

4.1 Cytoplasmic actins

Actins are highly conserved, abundant proteins found in nucleated cells of the eukaryotic genome, which play pivotal roles in many important cellular processes [32, 33]. In vertebrates, six isoforms namely skeletal muscle α-actin, cardiac muscle α-actin, smooth muscle α-actin, smooth muscle γ-actin, cytoplasmic β-actin and cytoplasmic γ-actin of actin have been isolated based on their tissue specificity [33]. Though individual genes encode each isoform, the cytoplasmic isoactins are only ~10% different from any of the muscle actins. Interestingly, the cytoplasmic isoactins β and γ differ at only 4 amino acid positions in the N-terminus of their 375 amino acids [33]. At the nucleic acid level, the cytoplasmic actins differ from each other at the 3'untranslated regions (UTRs) that are believed to be central to mRNA transcript localization in the cell [34]. In most cells the cytoplasmic β and γ isoactins are found in the constant ratio of 2:1 [33]. Studies have shown a spatial and temporal segregation of the cytoplasmic isoforms in different cell types, and until recently it was thought that the distribution of γ-actin was ubiquitous and not obviously related to function. β-actin distribution is dependent on the physiological function of the cell and is primarily found localized in the more dynamic structures of the cell such as the growth cone of differentiating neurons and the dendrites and axons of mature neurons [33, 35, 36].

The traditional functions of the ~43 kDa protein family include muscle contraction, cell motility, cell shape determination, exocytosis, endocytosis, cytokinesis and organelle transport. Recent research confirms the presence and importance of actin in the nucleus. Actin and actin-binding proteins are actively involved in gene expression, chromatin remodeling and pre-mRNA splicing of many nuclear genes [32]. In the cytoplasm, actin interacts with an unusually wide variety of interacting proteins to form higher order structures such as bundles or networks to perform various functions in the cell [32, 33]. Globular actin (G-actin), which is bound to ATP and/or ADP, polymerizes to form filamentous actin (F-actin) in the cell [33, 37, 38]. The F- actin in combination with myosins forms contractile fibrils (e.g. myofibrils of muscle), along with espin, fimbrin, or fascin forms densely packed non-contractile bundles (e.g. core bundles of stereocilia and microvilli) or forms gel-like networks (e.g. cuticular plate of hair cells, leukocytes cortex) in combination with α-actinin [39]. Actin polymerization has been extensively studied in the filopodia, lammelipodia and the dendritic spines of neurons [37, 38].

Actin filaments are helical polymers of G-actin subunits. These helical polymers consist of a barbed end and a pointed end. ATP-bound actin monomers are added to the barbed end while ADP-bound actin monomers dissociate from the pointed end. The actin polymer hence is polar in nature [38]. Actin binding and actin sequestering proteins like profilin bind to the ATP-G-actin pool in the cell, preventing spontaneous polymerization events [37, 38]. The

initial steps of monomer addition are unfavorable and occur slowly, while addition of subsequent monomers become favorable and the process proceeds rapidly [37, 38]. The growing actin filaments are characterized by continuous assembly (at the barbed end) and disassembly (at the pointed end), a process brought about by ATP-dependent hydrolysis of ATP in the filament [37]. Disassembly results from the disassociation of γ-phosphate (following ATP hydrolysis), which activates actin severing and debranching proteins, ultimately resulting in the disassociation of ADP-actin at the pointed end [37, 38]. This process of actin assembly and disassembly along the filaments is referred to as treadmilling or retrograde flow [37, 40] (Figure 1-7). Treadmilling is observed in the actin bundles of nerve growth cones, microvilli and newly formed stereocilia (reviewed in [41]). These rates vary from being ~1.5/s^{-1} in microvillar parallel actin bundles to ~2.5 times slower in stationary filopodia to ~ 5-50 times slower in *Listeria* comet tails [42]. For the actin bundle to continue treadmilling and maintain constant length, assembly of actin monomers at the barbed end and the disassembly at the pointed end of the filament should be tightly regulated [41]. Imbalance in these two processes can result in shorter or complete disappearance of the filaments. Though treadmilling is primarily regulated by two key proteins-ADF /cofilin, an actin depolymerizing factor and barbed end capping proteins (as shown in growth cones and lamellipodia), it is possible to imagine the pivotal roles of other actin binding proteins like myosins, and cross-linking proteins like espin [40, 41].

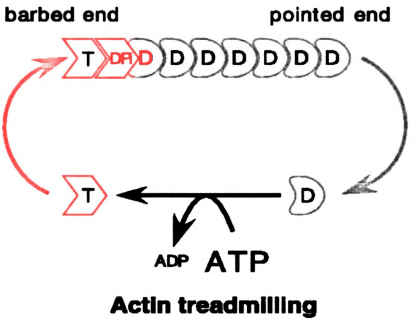

Figure 1-7: Treadmilling of actin filaments. ATP bound actin monomers are added at the barbed end, while ADP bound actin monomers dissociate from the pointed end. ATP-actin monomers move along the filament, with ATP moieties hydrolyzing to ADP and dissociation of γ-phosphate. This activates actin severing and debranching proteins which eventually cause the dissociation of ADP from pointed end (modified from [40]). This process of simultaneous addition and dissociation of actin monomers is termed treadmilling.

4.2 Regulation of actin cytoskeleton

Rho GTPases, members of the Ras super family of GTPases, are key regulators of actin cytoskeleton in many cell types [43, 44]. However proteins of the Ena/VASP family have been shown to be pivotal in actin assembly and cell motility. In various cell types these proteins were shown to localize to the tips of filopodia and edges of lammelipodia, which are regions of actin reorganization [45]. Ena/VASP family proteins contain an amino-terminal homology domain (EVH1), a proline-rich central region and a carboxy-terminal homology domain (EVH2). The proline- rich domain of all the family members contain binding sites for monomeric actin binding protein, profilin [45]. EVH2 domain contains a monomeric-actin-binding site, filamentous actin-binding site and an oligomerization facilitating coiled-coil site.

Ena/VASP family members act as barbed end de-capping proteins, thereby positively regulating actin filament lengths. In organisms like *Listeria,* these proteins bind directly to profilin at sites of actin organization and hence affect the rates of cell motility. They also perform the role of reducing actin filament branching events by possibly interfering with Arp2/3 complex [45]. Based on the data from my experiments (Chapter 2), it is possible that Ena/VASP proteins are critical in regulation of actin filament lengths in LLC-PK1-CL4 cells.

4.3 Actin in the ear

Three forms of actin filament cytoskeleton are found in the hair cells of vertebrates [39, 46]. These different actin filament assemblies include the extensively cross-linked actin bundles with uniform polarities of the stereocilia, gel-like actin networks of the cuticular plate, into which the base of stereocilia are anchored and the zonula adherens junction, that form a circumferential array of anti parallel actin filaments [10, 39, 46]. Actin filaments in stereocilia are cross-linked by fimbrin and espin, those in cuticular plate are cross-linked by spectrin while the filaments in zonula adherens are cross linked by α-actinin [39, 46].

Various studies have shown a spatial and temporal segregation of the cytoplasmic isoforms β and γ-actins in different cell types such as gastric parietal cells, osteoblasts, and neurons [33]. 2D gel electrophoresis followed by immunoblotting displayed, for the first time, the presence of both the cytoplasmic actin isoforms- β and γ in isolated sensory epithelium of chicken auditory cells [39]. Later studies showed similar results in the guinea pig hair cells [46]. The two cytoplasmic actin isoforms β and γ-actins are expressed in the stereocilia of hair cells and microvilli of the supporting cells [46].

In the chicken auditory hair cells β-actin expression is found only in the stereocilia and zonula adherens while γ-actin expression is seen in all the three actin rich structures of the inner ear: stereocilia, cuticular plate and zonula

adherens [39]. The current data suggest that γ-actin is the predominant isoform in the cochlea, unlike other major tissues [33, 39, 46]. In the guinea pig auditory cells, β-actin expression is detected in the cuticular plate but the levels are much less compared to the stereocilia and their rootlets [46]. γ-Actin expression on the other hand is more uniform along the stereocilia and the cuticular plate [46]. Recent work has shown that treadmilling occurs in the actin bundles of stereocilia as well, showing for the first time, that these actin bundles are highly dynamic structures [47, 48]. Though the specific function of each of the isoforms is not completely understood, data from rodents suggest that β-actin plays a role in maintaining the hair bundle structure [47].

4.4 γ-actin mutations and hearing loss

In 2003, novel mutations in the γ-isoform of cytoplasmic actin were identified by our lab and others as the cause of non-syndromic, autosomal progressive, late-onset, progressive hearing loss [21, 22, 49]. Recently, four more mutations (I122V, K118N, E241K and D51N) in γ-actin gene have been identified to cause non-syndromic progressive hearing loss [27-29].

The six missense mutations originally discovered were T89I, K118M, P264L, P332A, T278I and V370A [21, 22]. The mutations are found in evolutionarily conserved regions of the γ-actin gene and are distributed in 3 of 4 sub-domains of the protein (Figure 8). Based on their location, it is postulated

that these mutations might affect key actin processes like filament formation/polymerization (T278I, P264L), interaction with myosin (P332A, T89I, K118M), and bundling or gelation (T89I, K118M). Persons harboring these mutations exhibit similar phenotype and progression of hearing loss, with differences only in onset times [21]. In addition, mutations in this ubiquitously expressed protein cause only hearing loss. These observations indicate that γ-actin performs a very specific and pivotal role in hearing and suggests hair cell as the key target.

To investigate the affect of these mutations *in-vivo* and *in-vitro*, the six mutants were introduced into yeast actin [50]. Yeast cells harboring each of the mutant actins as the only copy of actin were found viable, but four mutants (K118M, T278I, P332A, and V370A) exhibited abnormal mitochondrial morphology. In addition, except T89I, the rest of the five mutants displayed abnormal vacuole formation. Biochemical analysis using purified mutant actins indicated that T89I, K118M and V370A were more susceptible to cofilin-induced disassembly, while P332A was more resistant [51]. In addition, V370A displayed abnormal actin polymerization [50].

The data from the yeast confirm that the missense mutations have a functional consequence for actin. However though informative, these findings do not provide a clear correlation with the deafness phenotype in humans [50]. Hence, investigation of these mutants in a vertebrate and mammalian model

system will be important to delineate their physiological effect. In this dissertation, a zebrafish model and a mammalian cell culture model system were explored to study the affect of the γ-actin mutations.

5 Espin

5.1 Distribution of espin isoforms

Espin (*ESPN*) was first identified in the ectoplasmic specializations of Sertoli cells of rat testis [52]. Immunogold labeling localized this novel actin-binding protein to the parallel actin bundles of ectoplasmic specializations [52]. A 2.9kb mRNA transcript encodes this 837-amino acid, 110kDa protein that showed specific localization to rat testis [52]. Later, multiple espin isoforms were detected in the brush border microvilli of rat intestine and kidney, dendritic spines of cerebellar purkinje fibers, and the actin bundles of many sensory cells like the hair cell stereocilia [42, 53-55]. Encoded by a single gene, the multiple isoforms arise from alternative transcriptional start sites and differential splicing [54, 55]. The longer 837-amino acid isoform contains 8 ankyrin-like repeats in its N-terminus, the 116 amino acid COOH-terminus carries an actin bundling module (ABM) [52, 55]. ABM has been shown to be necessary and sufficient to bundle actin filaments *in vitro* [56]. Besides ABM, there is an additional actin-binding (AB) site in the N-terminus, which makes espin two and half times more efficient at bundling actin filaments than other known actin-bundling proteins [57]. Unlike other actin-bundling proteins, espin is Ca^{2+} insensitive, another feature that makes espin an ideal actin-bundling protein in the hair cells [55]. The longer

isoform also contains two proline rich (PR1, PR2) regions and a WASP (Wiskott-Aldrich syndrome protein) homology (WH2) domain [55]. Espin binds to profilin (ATP-actin binding protein) via its proline rich domains and directly to monomeric actin via its WH2 domain. Recently, it was shown that the WH2 domain is capable of building actin bundles, when targeted to specific sites in the cells [58]. These data hint at a novel mechanism of actin bundling.

All the isoforms namely espin 1(found in Sertoli cells), espins 2A, 2B (expressed in Purkinje cells), espins 3A, 3B (found in sensory epithelium and retina) and 4 (expressed in the brush border of intestine and kidney) contain the ABM, encoded by 167 amino acid COOH-terminal peptide [53, 55]. Espins 2A, 2B, espins 3A, 3B and small espin 4, all lack the 8 ankyrin-like repeats in their N-terminal, while espins 3A, 3B and espin 4 do not contain a proline rich site and the additional actin binding site in the N-terminus [55]. When espin 3A and 3B isoforms were expressed in cell culture, they were found to localize to the actin bundles of microvilli and increased the average microvilli length from 1.33 ± 0.04 to 6.28 ± 0.09 and 6.04 ± 0.12 μm respectively [55]. These *in-vitro* data were validated when hair cell stereocilia of espin deficient jerker mice were studied [59].

5.2 ESPN mutations and hearing loss

Deaf jerker mice carry a recessive mutation in the espin gene that results in hair cell stereocilia degeneration resulting in hearing loss and vestibular dysfunction [60]. This spontaneously arising mutation results in a frame-shift in

the ABM of the C-terminal of espin protein, thereby creating an espin null. Fluorescence scanning confocal and electron microscopy studies were performed on the stereocilia of deaf jerker mice [59]. Espin deficient actin bundles of stereocilia were found to be shorter than the WT control stereocilia, which subsequently degenerated starting at post natal day 11, coinciding with the onset of hearing in mice [59, 60]. In addition, when espin was over-expressed in the neuroepithelial cells of organ of Corti cultures, lengthening of the actin bundles of stereocilia and microvilli was observed [59]. The above data establish espin as a pivotal protein for the growth and maintenance of stereocilia.

Recently, mutations in the espin gene (ESPN) were identified as the cause of autosomal recessive and dominant hearing loss in human populations [61-64]. Two frame-shift mutations, 1988delAGAG and 2469delGTCA, mapped to the actin-bundling module of the espin gene were shown to co-segregate with recessively inherited hearing loss and vestibular dysfunction in two consanguineous families [61]. A novel mutation, 1757insG, in the WH2 domain of the espin gene was determined to be the cause of recessively inherited congenital deafness without vestibular dysfunction [63]. Autosomal dominant mutations like D744N, R774Q and delK848 were mapped to the actin bundling module of espin protein [62]. Using an LLC-PK1-CL4 cell transfection model, it was shown that while D744N causes elongation of microvilli confined to small patches of the apical surface, delK848 severely impairs the elongation of microvilli, and R774Q does not show any effect [62]. Interestingly, the mutant

phenotypes observed in the cell culture model corresponded to the phenotype and severity of hearing loss in patients [62]. These data highlight the pivotal role of cell culture models in understanding the molecular biology of disease causing human mutant proteins.

6 LLC-PK1-CL4 transfection model

The pig proximal kidney epithelial cell line, LLC-PK-CL4 (CL4) forms a well-ordered brush order (BB) microvilli on its apical surface. CL4 cells have been successfully used to study the dynamics of cytoskeletal proteins like MYO1 A in these BB microvilli [65]. The parallel actin bundles in the microvilli are cross-linked by actin-bundling proteins like fimbrin/plastin and villin [66]. These cells lack endogenous expression of espin, the third actin-bundling protein. However, when differentiated CL4 cells are transfected with espin, the BB microvilli elongate to form long, spiky microvilli, without causing any other apparent morphological change in the cells [42]. These microvilli have been routinely used to study the biological properties/functions of the various espin isoforms and espin mutations causing hearing loss [55, 59, 62, 67, 68]. One such study showed that in espin expressing cells, the lengths of microvilli were dependent on the levels of espin expression [42]. Similar studies were performed on the deaf jerker mouse neuroepithelial cells of the organ of Corti cultures [59]. It was observed that in the absence of espin, stereocilia remain short while exogenous expression of espin results in lengthening of the stereocilia and microvilli.

In the context of studying hearing loss and genes involved in hearing loss, CL4 cells have become a valuable tool, especially in the absence of an animal model, in unraveling the role of important proteins that contribute to the structure of stereocilia, like actin and espin. In this thesis, the microvilli of CL4 cells have been used a model system to study the expression and functional properties of the γ-actin mutations.

7 Zebrafish as a model to study human hearing loss

Zebrafish has become an excellent model system to study human diseases [69]. Besides exhibiting rapid development and transparent embryos, many key factors that have made zebrafish a favorite model system include the ease of performing in-vivo imaging, transgenic knock-down, transgenic over-expression, small molecule screening, and chemical mutagenesis [69]. Thus human diseases like muscular dystrophies, myopathies, neurodegenerative diseases and cardiovascular disease have been vastly modeled in zebrafish [69-71].

For all the above-mentioned features, zebrafish has been an attractive model to study the function of genes involved in human hearing loss. *N*-Ethyl-*N*-nitrosourea (ENU) mutagenesis, has been successfully used to identify ~30 genes required for ear development [71]. Using zebrafish, it was shown that myosin VI is required for structural integrity of the apical surface of sensory hair

cells [72]. Zebrafish harboring mutations in many of these genes display 'circler' behavior, similar to the 'shaker' mice. There are zebrafish models of many human syndromic deafness disorders as well [71].

In addition to designing a cell culture model for the γ-actin mutations, we were successful in over-expressing the γ-actins in zebrafish. The details about the transgenic model will be elaborated in Chapter 3 of this thesis.

REFERENCES

1. Petit, C., J. Levilliers, and J.P. Hardelin, *Molecular genetics of hearing loss.* Annual Review of Genetics, 2001. **35**: p. 589-646.

2. Vrijens, K., L. Van Laer, and G. Van Camp, *Human hereditary hearing impairment: mouse models can help to solve the puzzle.* Human Genetics, 2008. **124**(4): p. 325-348.

3. Forge, A. and T. Wright, *The molecular architecture of the inner ear.* British Medical Bulletin, 2002. **63**: p. 5-24.

4. Wangemann, P., *K+ cycling and the endocochlear potential.* Hearing Research, 2002. **165**(1-2): p. 1-9.

5. Vlastarakos, P.V., et al., *Novel approaches to treating sensorineural hearing loss. Auditory genetics and necessary factors for stem cell transplant.* Medical Science Monitor, 2008. **14**(8): p. RA114-RA125.

6. Couloigner, V., O. Sterkers, and E. Ferrary, *What's new in ion transports in the cochlea?* Pflugers Archiv-European Journal Of Physiology, 2006. **453**(1): p. 11-22.

7. Raphael, Y. and R.A. Altschuler, *Structure and innervation of the cochlea.* Brain Research Bulletin, 2003. **60**(5-6): p. 397-422.

8. Nickel, R. and A. Forge, *Gap junctions and connexins in the inner ear: their roles in homeostasis and deafness.* Current Opinion In Otolaryngology & Head And Neck Surgery, 2008. **16**(5): p. 452-457.

9. DeRosier, D.J. and L.G. Tilney, *F-actin bundles are derivatives of microvilli: What does this tell us about how bundles might form?* Journal of Cell Biology, 2000. **148**(1): p. 1-6.

10. Tilney, L.G., M.S. Tilney, and D.J. Derosier, *Actin-Filaments, Stereocilia, and Hair-Cells - How Cells Count and Measure.* Annual Review of Cell Biology, 1992. **8**: p. 257-274.

11. Belyantseva, I.A., et al., *Stereocilia: the long and the short of it.* Trends in Molecular Medicine, 2003. **9**(11): p. 458-461.

12. Dallos, P., *Cochlear amplification, outer hair cells and prestin.* Current Opinion In Neurobiology, 2008. **18**(4): p. 370-376.

13. Belyantseva, I.A., et al., *gamma-Actin is required for cytoskeletal maintenance but not development.* Proceedings Of The National Academy Of Sciences Of The United States Of America, 2009. **106**(24): p. 9703-9708.

14. Bryant, J., R.J. Goodyear, and G.P. Richardson, *Sensory organ development in the inner ear: molecular and cellular mechanisms.* British Medical Bulletin, 2002. **63**: p. 39-57.

15. Rzadzinska, A.K., et al., *An actin molecular treadmill and myosins maintain stereocilia functional architecture and self-renewal.* Journal of Cell Biology, 2004. **164**(6): p. 887-897.

16. Frolenkov, G.I., et al., *Genetic insights into the morphogenesis of inner ear hair cells.* Nature Reviews Genetics, 2004. **5**(7): p. 489-498.

17. Cotanche, D.A., *Genetic and pharmacological intervention for treatment/prevention of hearing loss.* Journal Of Communication Disorders, 2008. **41**(5): p. 421-443.

18. Liu, X.Z. and D. Yan, *Ageing and hearing loss.* Journal Of Pathology, 2007. **211**(2): p. 188-197.

19. Brown, S.D.M., R.E. Hardisty-Hughes, and P. Mburu, *Quiet as a mouse: dissecting the molecular and genetic basis of hearing.* Nature Reviews Genetics, 2008. **9**(4): p. 277-290.

20. Petit, C., *From deafness genes to hearing mechanisms: harmony and counterpoint.* Trends In Molecular Medicine, 2006. **12**(2): p. 57-64.

21. van Wijk, E., et al., *A mutation in the gamma actin 1 (ACTG1) gene causes autosomal dominant hearing loss (DFNA20/26).* Journal of Medical Genetics, 2003. **40**(12): p. 879-884.

22. Zhu, M., et al., *Mutations in the gamma-actin gene (ACTG1) are associated with dominant progressive deafness (DFNA20/26).* American Journal of Human Genetics, 2003. **73**(5): p. 1082-1091.

23. Eisen, M.D. and D.K. Ryugo, *Hearing molecules: contributions from genetic deafness.* Cellular And Molecular Life Sciences, 2007. **64**(5): p. 566-580.

24. Strenzke, N., et al., *Update on physiology and pathophysiology of the inner ear. Pathomechanisms of sensorineural hearing loss.* Hno, 2008. **56**(1): p. 27-36.

25. Nance, W.E., *The genetics of deafness.* Mental Retardation and Developmental Disabilities Research Reviews, 2003. **9**(2): p. 109-119.

26. Nelson, E.G. and R. Hinojosa, *Presbycusis: A human temporal bone study of individuals with downward sloping audiometric patterns of hearing loss and review of the literature.* Laryngoscope, 2006. **116**(9): p. 1-12.

27. Morin, M., et al., *In vivo and in vitro effects of two novel gamma-actin (ACTG1) mutations that cause DFNA20/26 hearing impairment.* Human Molecular Genetics, 2009. **18**(16): p. 3075-3089.

28. de Heer, A.M.R., et al., *Audiometric and Vestibular Features in a Second Dutch DFNA20/26 Family With a Novel Mutation in ACTG1.* Annals Of Otology Rhinology And Laryngology, 2009. **118**(5): p. 382-390.

29. Liu, P., et al., *Novel ACTG1 mutation causing autosomal dominant non-syndromic hearing impairment in a Chinese family.* Journal Of Genetics And Genomics, 2008. **35**(9): p. 553-558.

30. Leibovici, M., S. Safieddine, and C. Petit, *Mouse Models Of Human Hereditary Deafness*, in *Mouse Models Of Developmental Genetic Disease*. 2008. p. 385-+.

31. Adams, A.E.M., D. Botstein, and D.G. Drubin, *A Yeast Actin-Binding Protein Is Encoded By Sac6, A Gene Found By Suppression Of An Actin Mutation.* Science, 1989. **243**(4888): p. 231-233.

32. Vartiainen, M.K., *Nuclear actin dynamics - From form to function.* Febs Letters, 2008. **582**(14): p. 2033-2040.

33. Khaitlina, S.Y., *Functional specificity of actin isoforms*, in *International Review of Cytology - a Survey of Cell Biology, Vol. 202.* 2001. p. 35-98.

34. Hoock, T.C., P.M. Newcomb, and I.M. Herman, *Beta Actin and Its Messenger-Rna Are Localized at the Plasma-Membrane and the Regions of Moving Cytoplasm During the Cellular-Response to Injury.* Journal of Cell Biology, 1991. **112**(4): p. 653-664.

35. Otey, C.A., et al., *Immunolocalization of the Gamma-Isoform of Nonmuscle Actin in Cultured-Cells.* Journal of Cell Biology, 1986. **102**(5): p. 1726-1737.

36. Hill, M.A. and P. Gunning, *Beta-Actin and Gamma-Actin Messenger-Rnas Are Differentially Located within Myoblasts.* Journal of Cell Biology, 1993. **122**(4): p. 825-832.

37. Pollard, T.D. and G.G. Borisy, *Cellular motility driven by assembly and disassembly of actin filaments (vol 112, pg 453, 2002).* Cell, 2003. **113**(4): p. 549-549.

38. Nicholson-Dykstra, S., H.N. Higgs, and E.S. Harris, *Actin dynamics: Growth from dendritic branches.* Current Biology, 2005. **15**(9): p. R346-R357.

39. Hofer, D., W. Ness, and D. Drenckhahn, *Sorting of actin isoforms in chicken auditory hair cells.* Journal of Cell Science, 1997. **110**: p. 765-770.

40. Pantaloni, D., C. Le Clainche, and M.F. Carlier, *Mechanism of actin-based motility (vol 292, pg 1502, 2001).* Science, 2001. **292**(5524): p. 2012-2012.

41. Tilney, L.G. and D.J. DeRosier, *How to make a curved Drosophila bristle using straight actin bundles.* Proceedings Of The National Academy Of Sciences Of The United States Of America, 2005. **102**(52): p. 18785-18792.

42. Loomis, P.A., et al., *Espin cross-links cause the elongation of microvillus-type parallel actin bundles in vivo.* Journal of Cell Biology, 2003. **163**(5): p. 1045-1055.

43. Hall, A., *Rho GTPases and the actin cytoskeleton.* Science, 1998. **279**(5350): p. 509-514.

44. Jaffe, A.B. and A. Hall, *Rho GTPases: Biochemistry and biology.* Annual Review Of Cell And Developmental Biology, 2005. **21**: p. 247-269.

45. Krause, M., et al., *ENA/VASP proteins: Regulators of the actin cytoskeleton and cell migration.* Annual Review Of Cell And Developmental Biology, 2003. **19**: p. 541-564.

46. Furness, D.N., et al., *Differential distribution of beta- and gamma-actin in guinea-pig cochlear sensory and supporting cells.* Hearing Research, 2005. **207**(1-2): p. 22-34.

47. Schneider, M.E., et al., *Structural cell biology: Rapid renewal of auditory hair bundles - The recovery time after noise-induced hearing loss is in step with a molecular treadmill.* Nature, 2002. **418**(6900): p. 837-838.

48. Manor, U. and B. Kachar, *Dynamic length regulation of sensory stereocilia.* Seminars In Cell & Developmental Biology, 2008. **19**(6): p. 502-510.

49. Rendtorff, N.D., et al., *A novel missense mutation in ACTG1 causes dominant deafness in a Norwegian DFNA20/26 family, but ACTG1 mutations are not frequent among families with hereditary hearing impairment.* European Journal Of Human Genetics, 2006. **14**(10): p. 1097-1105.

50. Bryan, K.E., et al., *Effects of human deafness gamma-actin mutations (DFNA20/26) on actin function.* Journal Of Biological Chemistry, 2006. **281**(29): p. 20129-20139.

51. Bryan, K.E. and P.A. Rubenstein, *Allele-specific Effects of Human Deafness gamma-Actin Mutations (DFNA20/26) on the Actin/Cofilin Interaction.* Journal Of Biological Chemistry, 2009. **284**(27): p. 18260-18269.

52. Bartles, J.R., A. Wierda, and L.L. Zheng, *Identification and characterization of espin, an actin-binding protein localized to the F-actin-rich junctional plaques of Sertoli cell ectoplasmic specializations.* Journal of Cell Science, 1996. **109**: p. 1229-1239.

53. Bartles, J.R., et al., *Small espin: A third actin-bundling protein and possible forked protein homolog in brush border microvilli.* Molecular Biology Of The Cell, 1998. **9**: p. 783.

54. Sekerkova, G., et al., *Novel espin actin-bundling proteins are localized to Purkinje cell dendritic spines and bind the Src homology 3 adapter protein insulin receptor substrate p53.* Journal Of Neuroscience, 2003. **23**(4): p. 1310-1319.

55. Sekerkova, G., et al., *Espins are multifunctional actin cytoskeletal regulatory proteins in the microvilli of chemosensory and mechanosensory cells.* Journal of Neuroscience, 2004. **24**(23): p. 5445-5456.

56. Bartles, J.R., et al., *Espin is the missing crosslinker in the actin bundles of hair cell stereocilia.* Molecular Biology of the Cell, 1998. **9**: p. 135A-135A.

57. Chen, B., et al., *Espin contains an additional actin-binding site in its N terminus and is a major actin-bundling protein of the Sertoli cell-spermatid ectoplasmic specialization junctional plaque.* Molecular Biology of the Cell, 1999. **10**(12): p. 4327-4339.

58. Loomis, P.A., et al., *Targeted wild-type and jerker espins reveal a novel, WH2-domain-dependent way to make actin bundles in cells.* Journal Of Cell Science, 2006. **119**(8): p. 1655-1665.

59. Rzadzinska, A., et al., *Balanced levels of espin are critical for stereociliary growth and length maintenance.* Cell Motility and the Cytoskeleton, 2005. **62**(3): p. 157-165.

60. Zheng, L.L., et al., *The deaf jerker mouse has a mutation in the gene encoding the espin actin-bundling proteins of hair cell stereocilia and lacks espins.* Cell, 2000. **102**(3): p. 377-385.

61. Naz, S., et al., *Mutations of ESPN cause autosomal recessive deafness and vestibular dysfunction.* Journal Of Medical Genetics, 2004. **41**(8): p. 591-595.

62. Donaudy, F., et al., *Espin gene (ESPN) mutations associated with autosomal dominant hearing loss cause defects in microvillar elongation or organisation.* Journal of Medical Genetics, 2006. **43**(2): p. 157-161.

63. Boulouiz, R., et al., *A Novel Mutation in the Espin Gene Causes Autosomal Recessive Nonsyndromic Hearing Loss But No Apparent Vestibular Dysfunction in a Moroccan Family.* American Journal Of Medical Genetics Part A, 2008. **146A**(23): p. 3086-3089.

64. Naz, S., et al., *A mutation of ESPN causes autosomal recessive nonsyndromic hearing loss, DFNB36.* American Journal Of Human Genetics, 2002. **71**(4): p. 1995.

65. Tyska, M.J. and M.S. Mooseker, *MYO1A (brush border myosin I) dynamics in the brush border of LLC-PK1-CL4 cells.* Biophysical Journal, 2002. **82**(4): p. 1869-1883.

66. Bartles, J.R., *Parallel actin bundles and their multiple actin-bundling proteins.* Current Opinion In Cell Biology, 2000. **12**(1): p. 72-78.

67. Li, H.W., et al., *Correlation of expression of the actin filament-bundling protein espin with stereociliary bundle formation in the developing inner ear.* Journal of Comparative Neurology, 2004. **468**(1): p. 125-134.

68. Sekerkova, G., et al., *Espins and the actin cytoskeleton of hair cell stereocilia and sensory cell microvilli.* Cellular And Molecular Life Sciences, 2006. **63**(19-20): p. 2329-2341.

69. Ingham, P.W., *The power of the zebrafish for disease analysis.* Human Molecular Genetics, 2009. **18**: p. R107-R112.

70. Chico, T.J.A., P.W. Ingham, and D.C. Crossman, *Modeling cardiovascular disease in the zebrafish.* Trends In Cardiovascular Medicine, 2008. **18**(4): p. 150-155.

71. Whitfield, T.T., *Zebrafish as a model for hearing and deafness.* Journal Of Neurobiology, 2002. **53**(2): p. 157-171.

72. Seiler, C., et al., *Myosin VI is required for structural integrity of the apical surface of sensory hair cells in zebrafish.* Developmental Biology, 2004. **272**(2): p. 328-338.

CHAPTER 2

Mutations in cytoplasmic γ-actin interfere with actin assembly dynamics

Abstract

Mutations in cytoplasmic γ-actin cause non-syndromic, post-lingual, autosomal-dominant, progressive sensorineural hearing loss. LLC-PK1- CL4 cells provide a model system to study the distribution of actins and the role of γ-actin and its mutations in repair of damaged structures like microvilli. Immunohistochemistry and confocal localization studies showed that β-actin was found primarily at the periphery of cells while γ-actin is abundant in the perinuclear space and cytoplasm of the cell. Exogenous expression of mutant γ-actins showed distribution to all the actin structures in the cell; the periphery, stress fibers and perinuclear space. In response to exogenous espin, filamentous mutant actins co-localized with espin in the microvilli. Co-transfection of espin and mutant actin resulted in each of the mutants co-localizing with filamentous actin in the microvilli. Cytochalasin D treatments of WT γ-actin and mutant γ-actins showed no difference in the repair of the damaged microvilli. Measurements of the lengths of microvilli however indicated that the microvilli expressing mutant actins were ~20-25% shorter than the WT γ-actin microvilli. Quantitative FRAP assays did not reveal any differences in the recovery rates between WT and mutants actins. Our data suggest that mutations in γ-actin exhibit subtle phenotypes and might interfere with basic actin assembly dynamics.

Introduction

Actin is a ubiquitously expressed eukaryotic protein which plays a key role in muscle contraction, cell motility, cell shape determination, exocytosis, endocytosis, cytokinesis and organelle transport [1, 2]. The distribution and function of actin in the cell is primarily governed by the requirements of the cell and various actin-binding proteins. Actin- filament binding proteins control processes like nucleation, assembly, disassembly and cross-linking, while actin-monomer binding proteins like profilin, ADF/cofilin etc regulate the pool of monomeric actin in the cell.

Three subtypes of actin (α,β and γ) have been described in humans, based on their mobility on 2D gels [1]. Six isoforms of actin have been identified based on their relative abundance in specific tissues. The two cytoplasmic isoactins β and γ, encoded by *ACTB* and *ACTG1* respectively, differ at only 4 amino acid positions in the N-terminus of their 375 amino acids. In most cells, β and γ isoactins are found in the constant ratio of 2:1. However, cells such as human erythrocytes primarily contain β-actin while in brush border cells from intestinal epithelium, as well as hair cells of the inner ear, γ-actin predominates. Studies from various laboratories have shown a spatial and temporal segregation of the cytoplasmic isoforms in different specialized cell types such as gastric parietal cells, hair cells, osteoblasts and neurons [1, 3, 4].

The only mutations in cytoplasmic γ-actin described to date are missense mutations that cause non-syndromic autosomal-dominant hearing loss. Our lab and others described the first mutations in γ-actin to cause autosomal-dominant, progressive, post-lingual sensorineural hearing loss (SNHL) [5, 6], and subsequently more mutations have been identified [7, 8] . This finding, though not surprising considering the central role of γ-actin in the inner ear, is nevertheless perplexing. Hearing loss is the only phenotype in individuals carrying mutations in γ-actin, which is a highly conserved and ubiquitously expressed protein. We hypothesize that γ-actin plays a very specific role in the inner ear.

Stereocilia, which are key players in the process of hearing, are filamentous actin filled structures found on the apical surface of hair cells [9, 10]. In mammals, these actin filaments are bundled into paracrystalline structures by actin-bundling proteins fimbrin and espin [9]. Espin isoforms, encoded by a single gene, are actin-bundling proteins that are found in brush border microvilli, hair cell stereocilia and the actin rich dendritic spines of Purkinje cells [11, 12]. In chicken hair cells, espin expression is observed as early as E8. Espin continues to be expressed in matured stereocilia-suggesting a role of espin in maintaining the hair bundle structure [13]. Spontaneous mutations in espin cause shortening of stereocilia resulting in vestibular dysfunction and deafness-further indicating a pivotal role played by espin in stereociliary length maintenance [14].

Stereocilia are derivatives of actin-filled microvilli found on the surface of hair cells [10]. The pig proximal kidney epithelial cell line, LLC-PK1-CL4 (CL4), upon cell-cell contact differentiates to form well-ordered brush border (BB) microvilli on its apical surface [15]. Owing to the highly ordered filamentous actin array of microvilli, CL4 cells are an excellent model system for studying the dynamics of BB microvilli and the cytoskeletal proteins. CL4 cells do not express espin endogenously, but make long spiky actin rich microvilli in response to exogenous espin. Of the six initially identified γ-actin mutations (T89I, K118M, P264L, P332A, T278I, V370A), two of them (T89I, K118M) are located in predicted interaction sites for actin bundling proteins (Figure 2-1). Hence we chose CL4 cells as the model system. In addition, due to the structural similarities between stereocilia and microvilli, CL4 cells were an ideal model system to study the effect of mutations in γ-actin.

Here we show that exogenous expression of all the mutant actins resulted in their localization to cell body, stress fibers and cell periphery. Mutant actins co-localized with espin in the microvillar structures. However, expression of the mutant proteins results in the shorter microvilli. Fluorescence Recovery After Photobleaching (FRAP) of the microvilli expressing mutant γ-actins showed that two of the six mutants have a higher proportion of mobile fractions. This finding suggests that γ-actin mutants possibly interfere with basic actin filament processes.

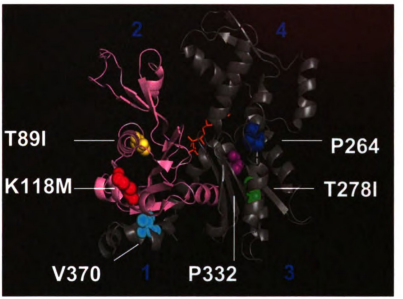

Figure 2-1: Ribbon structure model representing the location of γ-actin mutations. γ-Actin consists of two domains (represented by two different ribbon colors), which are further divided into 4 sub-domains (1,2,3,4 in blue). The six initially identified mutations of γ-actin are located throughout the molecule. T89I and K118M are located in sub-domain 1, in the predicted actin-bundling domain. Modified from [16].

Materials and Methods

Cell line: Pig kidney proximal tubule epithelial cell line LLC-PK1-CL4 (CL4) cells were a kind gift from James R. Bartles at Northwestern University, Chicago. The cells were maintained in DMEM, supplemented with 10% serum and 100mM L-glutamine.

Plasmid Constructs: The coding sequence of human WT and the six mutant γ-actins were cloned into Xho1/BamH1 sites of pEGFP-Actin vector (Clontech Inc). pEGFP-C2-espin2B construct was a kind gift from James R. Bartles at Northwestern University, Chicago. Thom Friedman at NIDCD kindly provided pDsRed-Monomer C1 vector. Espin, WT and mutant γ-actins were cloned into the Xho1/BamH1 sites of pDsRed Monomer C1 vector. WT and mutants actins were under a CMV promoter in all the plasmid constructs.

Immunohistochemistry: CL4 cells were plated on coverslips on day 0. On day 1, cells were fixed in cold 100% methanol at –20°C for 15 min followed by 3 washes in 1XPBS. Cells were blocked in 5% goat serum + 2% BSA at RT for 20 min. Cells were then incubated at RT for 2 hrs in 1:500 and 1:100 dilutions of γ-actin and -actin antibody respectively (γ antibody developed by our lab, β antibody from AbCam). Cells were washed with 1XPBS, 3 times for 5 min each. Cells were then incubated in 1:200 dilutions of FITC and cy3 tagged secondary antibodies, with shaking in dark, at RT for 30 min. Following a wash in 1XPBS for 10 min, coverslips were air dried and mounted.

Transient Transfections and Stable Line Generation: ~$8X10^6$ cells were plated on a cover slip on day 0.1μg DNA each of GFP and DsRed tagged plasmids were

transfected on day 2 using fugene transfection reagent (Invitrogen). 24 hours post transfection, cells were fixed in 4% paraformaldehyde (PFA) for 20 min at RT. Cells were then washed in 1XPBS and permeabilized with 0.1%Triton-X100 for 5 min. Cells were blocked in 1% BSA for 30 min at RT, stained with DAPI (1:10,000 dilution) for 5 min at RT, and washed in ddH20 for 10 min. The cover slip was air dried and mounted on a slide using fluoroguard anti-fade reagent (Bio-Rad). For stable cell line generation, cells were similarly plated and transfected. Following day of transfection, the media was replaced with media containing 100mg/ml G418 selection drug. The media was changed everyday, replacing with fresh media containing G418. After ~1.5 weeks, sterile cloning cylinders were used to pick the clones that were resistant to G418. These clones were transferred into a 12 well plate and grown in G418 medium from that point onwards.

Confocal Microscopy: Cells were viewed under Olympus Fluoview 1500 confocal microscope. Images were taken under 60X PlanApo objective and 3.5 digital magnification. The lengths of the microvilli were measured using the Olympus 1500 software.

FRAP assays: Cells were plated on glass-bottom dishes (MatTek Inc) on day 0. On day 1, cells were transfected with 1ug each of EGFP-actin (WT/mutant) and DsRed-espin. FRAP was performed on the microvilli of the transfected cells on day 2 using Olympus 1500 confocal microscope. Cells were placed in a 37°C chamber, with phenol red free 10% DMEM media containing 25 mM HEPES to maintain pH. The cell was scanned 10 times (at 1% 488 argon laser intensity),

and the 10^{th} scan was considered as pre-bleach. Region of interest (ROI) of microvilli were bleached at 70% laser intensity for 3 seconds. ROIs showing 55-70% bleach were used for further analysis. Fluorescence recovery scans were performed 30 seconds apart, with the first scan immediately following the bleach period, over a period of 4.5 minutes, at 1% laser intensity. Metamorph software (Molecular Devices) was used to calculate background intensity for each cell over each time point. This software was used to calculate the intensity of an adjacent fluorescent cell at each time point, to confirm that the cell undergoing FRAP was not bleaching as a consequence of scanning. A stringent method was developed where cells that bleached only 55-70% were considered. Mobile fractions were then calculated using Metamorph and KaleidaGraph softwares [32].

Statistical Analysis: Students t-test, using one-tailed distribution and two-sample equal variance, was used to determine the statistical significance between the microvilli lengths of WT and mutant γ-actins. Similar conditions were used to determine statistical significance for FRAP assays. Data from 3 independent experiments were combined together to obtain the final n for the microvilli length experiments. Due to the large number (~192) of n in individual experiments, it was possible to combine the 3 experiments.

Results

Endogenous actin distribution

The distribution and localization of endogenous cytoplasmic actin isoforms (β,γ) in CL4 cells is unknown. We investigated the isoform specific distribution of endogenous actin before over-expressing exogenous actin. Antibodies specific to β-and γ-actin isoform were used to perform immunocytochemistry. As shown in Figure 2-2A&B, in spreading cells, β-actin is primarily observed in the stress fibers, and along the periphery. In contrast, γ-actin (Figure 2-2B&C) is enriched in the cell body (perinuclear space) and the stress fibers. Our data suggest a possible differential role of β and γ-actins in CL4 cells similar to that described in other cell lines and tissues [1, 17, 18]. In confluent cells, I do not observe any difference in the distribution and localization of β and γ-actins in the cell periphery and perinuclear space, but there is more γ-actin in the cell body like in spreading cells (Figure 2-2D-F).

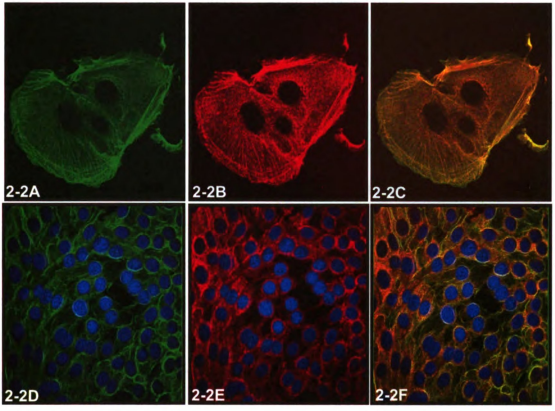

Figure 2-2: Spatial distribution of endogenous cytoplasmic actins in LLC-PK1-CL4 cells. β-Actin specific antibody (AbCam) and γ-actin specific primary antibodies were used to stain for the actins. Cells were fixed in 100% methanol at –20C and imaged under Olympus 1500 confocal microscope, 60X PlanApo objective. **2-2A,D**: β-Actin secondary antibody is FITC tagged, while γ-actin secondary antibody is rhodamine tagged **(2-2B,E)**. In spreading cells, β-Actin is found along the periphery and in stress fibers, γ-actin is primarily found in the perinuclear space and stress fibers **(2-2C)**. In confluent cells, there is no observable difference in the actin isoform distributions along cell periphery, but more γ-actin is observed in the cell body compared to β-actin **(2-2D-F)**. Cells here are counter stained with DAPI for the nucleus. Bar: 10μm

Exogenous expression of wild-type (WT) and mutant actins

Human WT β and γ-actin and all the original six mutants described for γ-actin were cloned into N-terminal tagged pEGFP vector and individually expressed in CL4 cells, under the control of the CMV promoter. Over expression of cytoplasmic actins has been reported to cause gross morphological changes in many cell types [17]. This observation is not surprising as actin plays a critical role in many physiologically important processes like motility, intracellular and organelle trafficking. Exogenous over expression could disrupt these critical processes. Hence it was important to determine if over expression of WT actins in CL4 cells would be detrimental to the cells. As seen in Figure 2-3A and 2-3B, exogenous expression of either β-actin or γ-actin did not affect the gross cell morphology. Both the proteins were seen in stress fibers, along the cell periphery and in all the expected actin rich structures. Cells expressing these actins continued to look healthy at least 72 hrs post transfection (data not shown).

To determine the effect of hearing loss mutations on the distribution of γ-actin, the six γ-actin mutants were individually expressed in the CL4 cells. All the six mutants (Figure 2-4B-G) localized to all actin rich structures in the cell and were indistinguishable from the WT control (Figure 2-4A).

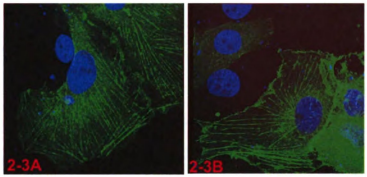

Figure 2-3: Exogenous-expression of cytoplasmic actins in LLC-PK1-CL4 cells. N-terminal EGFP tagged β and γ-actins were over-expressed using a CMV promoter in the CL4 cells. 24hrs post transfection, the cells were fixed in 4% paraformaldehyde (PFA), counter stained with DAPI for nucleus and imaged under Olympus 1500 confocal microscope, 60X PlanApo objective. **2-3A**: EGFP-β-actin localized to the periphery and stress fibers. **2-3B**: EGFP-γ-actin also localized to the periphery and stress fibers. No morphological changes were observed in the cells over-expressing cytoplasmic actins. Bar: 20μm

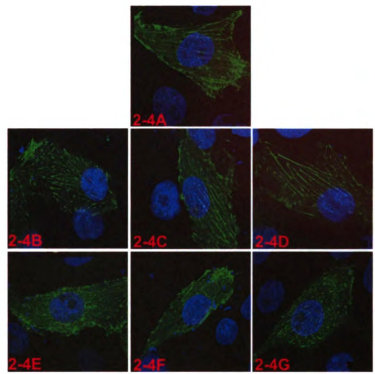

Figure 2-4: Over-expression of γ-actin mutants in LLC-PK1-CL4 cells. N-terminal EGFP- tagged γ-actin mutations were over-expressed, under the CMV promoter, to determine their distribution and localization in CL4 cells. 24 hrs post transfection, the cells were fixed in 4% PFA and counter stained with DAPI (blue) to label DNA. They were imaged under Olympus 1500 confocal microscope, 60X PlanApo objective. All the six mutants (**2-4B-G**) localized to actin-rich stress fibers, were found along the periphery of the cell and in the perinuclear space, and were indistinguishable from the WT control (**2-4A**). 2-4A: EGFP-WT γ-actin, 2-4B: EGFP-T89I, 2-4C: EGFP-K118M, 2-4D: EGFP-P264L, 2-4E: EGFP-P332A, 2-4F: EGFP-T278I, 2-4G: EGFP-V370A

Expression and localization of espin, WT, and mutant actins

The stereociliary bundles found on the surface of hair cells contain parallel bundles of filamentous actin. In the mammalian stereocilia, actin-bundling proteins like espin and fimbrin maintain these paracrystalline bundles [10]. Considering the pivotal role of espin in actin- bundling and in hearing, we set out to determine if γ-actin mutants were defective in localizing/binding to espin, thereby possibly resulting in weaker filaments. To verify the CL4/espin response, we demonstrated that expression of espin results in the lengthening of brush border microvilli in these epithelial cells [19] (Figure 2-5). Hence, CL4 cells are an excellent system to study microvillar localization properties of WT and γ-actin mutants.

Co- transfection of DsRed-espin and GFP-WT γ-actin resulted in co-localization of actin and espin in the microvilli with concomitant lengthening (Figure 2-6A). Co-transfection of DsRed-espin and each of the mutant γ-actins also resulted in the mutant actins co-localizing with espin in the microvilli (Figure 2-6B-G).

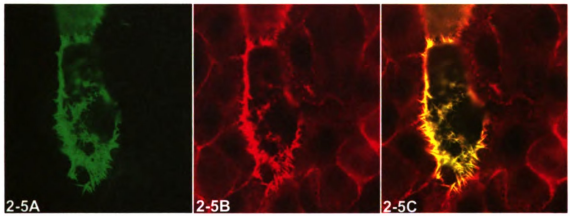

Figure 2-5: Exogenous expression of espin results in lengthening of brush border microvilli actins in LLC-PK1-CL4 cells. N-terminal EGFP-tagged espin plasmid was transfected into ~90 % confluent cells. 24 hrs post transfection, the cells were fixed in 4% PFA and imaged under Olympus 1500 confocal microscope, 60X PlanApo objective. **2-5A**: Over-expression results in the formation of long spiky microvilli. **2-5B**: The cells were counter stained with rhodamine phalloidin to label filamentous actin. **2-5C**: A merge of the images confirms co-localization of espin and actin. Bar: 10μm

Figure 2-6: Localization of WT or mutant γ-actins with espin in LLC-PK1-CL4 cells. Confluent cells were transfected with N-terminal EGFP-tagged espin and either DsRed- tagged WT or each of the six mutant γ-actins. 24 hrs post transfection, cells were fixed in 4% PFA and imaged under Olympus 1500 confocal microscope, 60X PlanApo objective. **2-6A**: WT γ-actin co-localizes with espin in the microvilli of CL4 cells. **2-6B-5G**: All the six mutants also co-localize with espin in the microvilli. Compared to WT-γ-actin, mutant actins do not show any difference in the distribution or co-localization with espin. Bar: 10μm

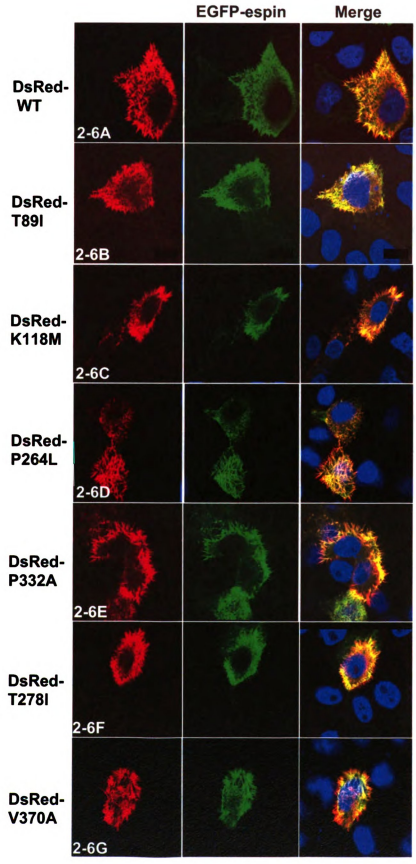
EGFP-espin
Merge
DsRed-WT
2-6A
DsRed-T89I
2-6B
DsRed-K118M
2-6C
DsRed-P264L
2-6D
DsRed-P332A
2-6E
DsRed-T278I
2-6F
DsRed-V370A
2-6G

Expression of γ-actin mutants results in shorter microvilli

The lengths of espin induced microvilli are proportional to the level of espin expression in the CL4 cells [19]. To determine the effects of actin mutations on microvilli length, a cell line constitutively expressing EGFP-espin was established. This stable cell line was then transfected with DsRed-actin mutations expression constructs. On careful analysis of the microvilli, we observed that the cells expressing γ-actin mutations had shorter microvilli compared to the cells expressing WT γ-actin (Figure 2-7A). Briefly, 12 transfected cells for each mutation were imaged and 16 microvilli per cell were measured (n=~195). Each experiment was repeated at least 3 times (T278I was done twice). To further confirm that the microvilli lengths were shorter due to mutant actin over expression, microvilli of neighboring untransfected cells in each case were measured and compared to the microvilli lengths of neighboring untransfected cells of WT γ-actin transfection. As expected, the lengths of microvilli of the mutant untransfected cells were comparable to that of WT untransfected cells (Figure 2-7B) and longer than their mutant actin transfected neighbors. Also, the microvilli in cells expressing WT γ-actin and those of neighboring untransfected cells were not significantly different, thereby demonstrating that the expression of exogenous actin itself does not cause microvilli shortening (Figure 2-7C).

Figure 2-7: Over-expression of mutant γ-actin results in shorter microvilli. DsRed-WT or DsRed-mutant γ-actins were individually over-expressed in EGFP-espin stable cell line. The cells were fixed in 4% PFA and imaged under Olympus 1500 confocal microscope, 60X PlanApo objective. In each case, 12 cells expressing the actin construct were imaged. 16 microvilli per cell were measured. The mean lengths of WT and mutant actins were calculated and students t-test was performed to determine if the difference in the lengths between mutants and WT was significant. Standard deviations are shown for each data set. **2-7A**: n=3 (12 cells x 16 microvilli x 3 = 576 microvilli). The means from 3 independent experiments were pooled and the graph was plotted. The microvilli expressing mutant actins were ~20-25% shorter than their WT control. **2-7B**: The maximum intensity projection image (of a Z series) of DsRed- WT-γ-actin expressing cell in EGFP-espin stable cell line. **2-7C**: The maximum intensity projection (of a Z series) of one of the mutants (Dsred-T89I-γ-actin) expressing cell in EGFP-espin stable cell line. Microvilli of cells expressing the mutant actin are shorter than the microvilli of cells expressing WT -γ-actin. **2-7D**: To further confirm this data, untransfected cells in each set were imaged and their microvilli were measured. n=1,WT-transfected: mean of 3 experiments. The lengths of microvilli of cells not expressing the mutant actins were no different than the lengths of microvilli of cells not expressing the WT-actin. In addition, the lengths of microvilli expressing WT-actin were same as the lengths of microvilli of cells not expressing the mutant actins further confirming that over-expression of WT actin does not result in shorter microvilli.

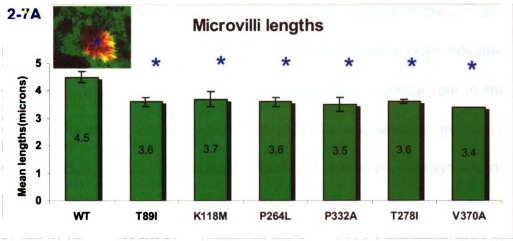
2-7A
Microvilli lengths
Mean lengths(microns)
5
4
3
2
1
0
4.5
3.6
3.7
3.6
3.5
3.6
3.4
WT
T89I
K118M
P264L
P332A
T278I
V370A

*p< 0 .0001

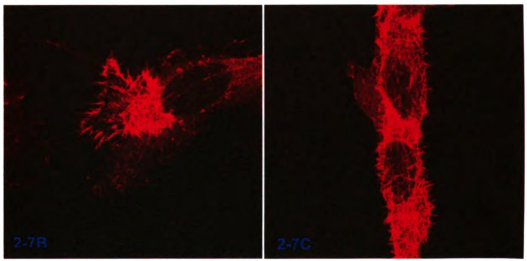
2-7B
2-7C

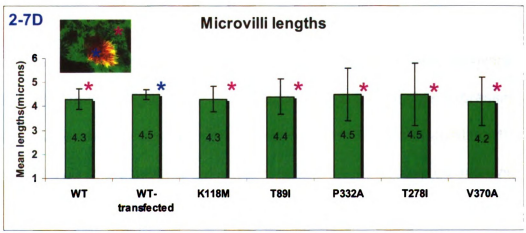
2-7D
Microvilli lengths
Mean lengths(microns)
6
5
4
3
2
1
4.3
4.5
4.3
4.4
4.5
4.5
4.2
WT
WT-transfected
K118M
T89I
P332A
T278I
V370A

Cytochalasin D treatments of γ-actin expressing microvilli

Persons harboring γ-actin mutations develop hearing loss in the 2nd and 3rd decade [5, 6]. Recent data from a γ-actin knock-out mouse model indicates that γ-actin is not involved in development, but might play a critical role in the maintenance and /or repair of actin structures [20]. To test whether mutant γ-actins are impaired in repair, low concentrations of the actin depolymerizing agent cytochalasin D (CD) was used to simulate damage and subsequent repair. Two mutations, T89I and K118M were chosen for this experiment since they lie in the predicted actin-bundling interaction domain of actin. Thus any defects, if observed in the repair process, could be attributed to poor binding of the mutants to espin. Briefly, CL4 cells stably expressing espin and transiently expressing EGFP tagged actins (WT or T89I or K118M) were treated with 100 nM of CD for 13 hrs. Low concentrations of CD result in shortening of actin filaments [19] but the affect is reversible. Following cytochalasin D treatment, the cells were allowed to recover for 4 1/2 hrs. The lengths of the microvilli of untreated and recovered microvilli were measured using the Olympus 1500 confocal microscope.

I did not observe any difference in the lengths of untreated and recovered microvilli in the mutants (Figure 2-8). The recovered microvilli of cells expressing the mutants were not any shorter than the untreated microvilli. In addition, the recovered microvilli of the mutants remained shorter than the recovered microvilli

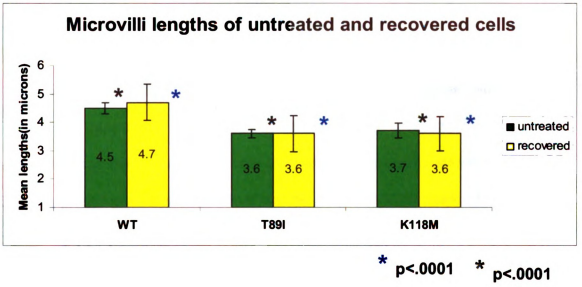

Figure 2-8: Microvilli lengths in cells before and after cytochalasin D treatment. EGFP-espin stable cell line was transfected with either DsRed-WTγ-actin or T89I or K118Mγ-actin mutants. Following transfections, cells were treated with 100 nM cytochalasin D for 13hrs. Cytochalasin D was removed from the media and cells were allowed to recover for 4.5 hrs. Microvillar lengths were measured before cytochalasin D treatment and after 4.5 hrs of recovery. In WT and mutant cells, there was no difference in the microvillar lengths between the untreated and recovered cells. The mutant microvilli were as long as their untreated counter parts. Like the untreated microvilli (Figure 2-6A), mutant recovered microvilli were also significantly shorter than WT recovered microvilli.

of WT γ-actin (like the untreated microvilli lengths). Since no difference in the recovery rates were observed in two mutants, this assay was not performed on the other 4 mutants.

FRAP assays to determine protein mobility

It is evident from various experiments that the physiological role of actin in the cell is dependent on numerous actin-binding proteins [2, 21]. Actin treadmilling has been shown to occur in microvilli and young stereocilia [19, 22, 23]. This phenomenon is dependent on the polymerization rates of monomeric actin and depolymerization of filamentous filaments. Monomeric actin-binding protein profilin and filament severing protein cofilin are pivotal for filament polymerization and depolymerization rates [21, 24]. Espin and myosin XVa, actin-binding proteins, are critical for lengthening of stereociliary bundles [25, 26]. Recent biochemical experiments performed on purified mutant γ-actins showed that the mutant actins exhibited various degrees of sensitivities to cofilin binding [27].

Based on our data and what is reported in literature, we hypothesized that the cause of shorter microvilli could be due to impaired actin protein trafficking or filament incorporation. To this end, I performed fluorescence recovery after photobleaching assays on the microvilli of cells expressing mutant actins. Briefly, cells are scanned 10 times, before an area of microvilli is bleached. The 10^{th}

scan is considered the prebleach scan. Microvilli are bleached for ~3 seconds at 70% laser intensity. Recovery scans were performed every 30 seconds for ~4.5 minutes. Figure 2-9A shows an entire series of WT γ-actin cell undergoing FRAP. Using Metamorph imaging software (Molecular Devices) and KaleidaGraph software (Synergy Software), the mobile fraction for WT and each of the mutants was calculated. For each scan, a background value (region not expressing EGFP) and a value from an adjacent cell expressing EGFP is calculated. These values are essential for calculating the mobile fraction.

Recovery graphs of WT γ-actin and the six mutants were plotted. Mobile fraction is an indicator of the availability of the protein being studied. No significant difference between the mobile fractions of WT and mutant actins was observed (Figure 2-9C-9H). Figures 2-10A-F are representative images of pre-bleach, bleach and recovered cells (after 4.5') of each of the mutants following FRAP.

Figure 2-9A-B: Fluorescence recovery after photobleaching of EGFP-WT γ-actin. 2-9A: The cell was scanned 10 times, without any interval between the scans, to obtain the prebleach image (image following the 10^{th} scan). A region of the microvilli is then bleached for ~3 seconds at 70% laser intensity. This is the bleach image. Following the bleach, the entire cell is scanned every 30 seconds to obtain the recovery images. The recovery was performed for ~4.5 minutes. **2-9B:** A representative graph is shown, where recovery of the region of interest (ROI), adjoining cell (CF) and background (BG) fluorescence are plotted.

2-9A

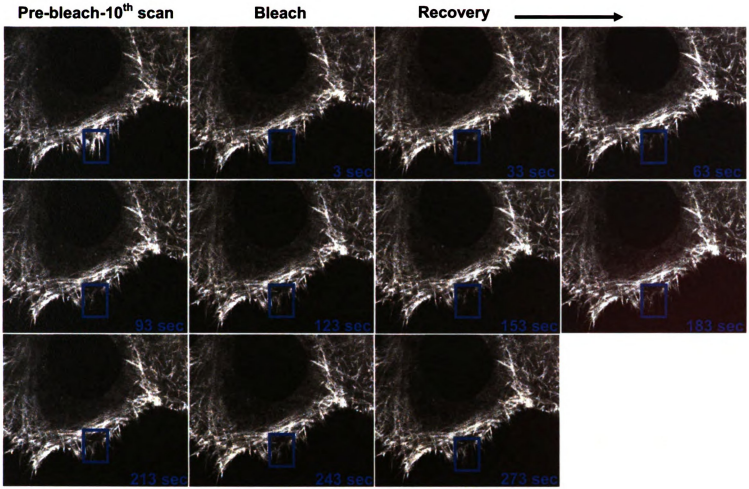
Pre-bleach-10th scan
Bleach
Recovery
3 sec
33 sec
63 sec
93 sec
123 sec
153 sec
183 sec
213 sec
243 sec
273 sec

2-9B

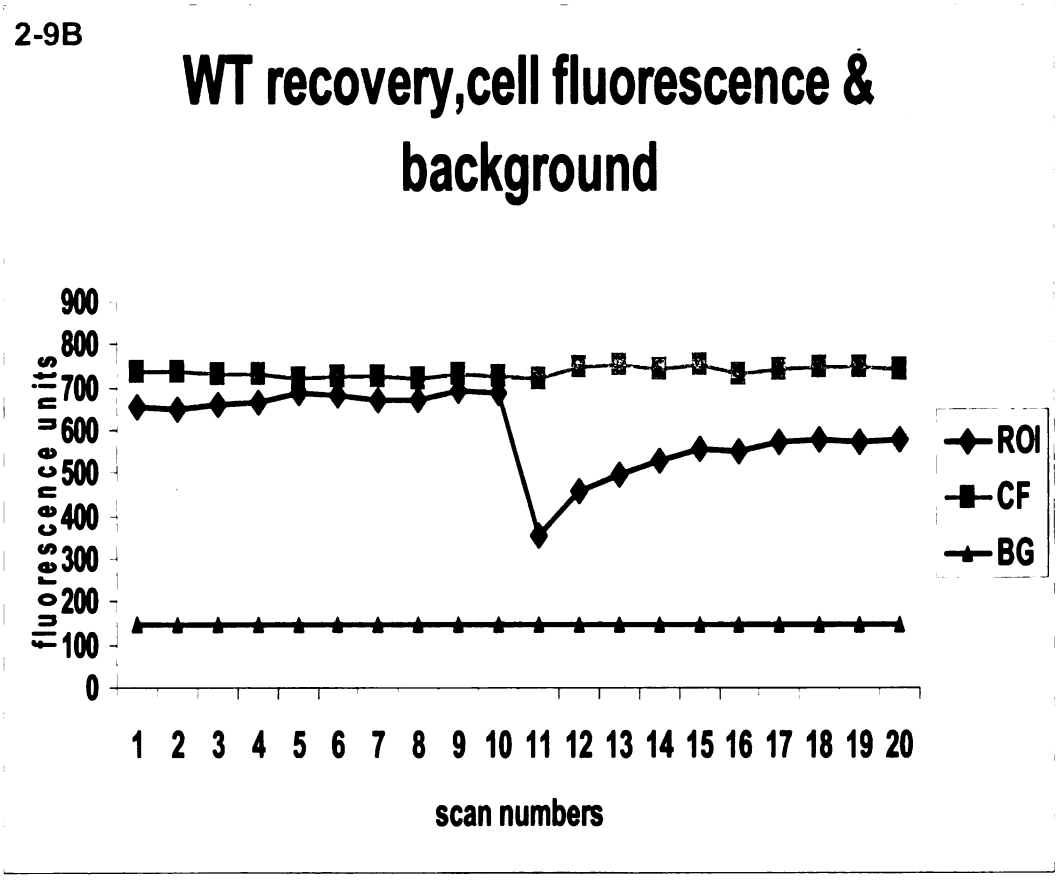
WT recovery,cell fluorescence & background
fluorescence units
900
800
700
600
500
400
300
200
100
0
1 2 3 4 5 6 7 8 9 10 11 12 13 14 15 16 17 18 19 20
scan numbers
ROI
CF
BG

Figure 2-9C-2-9H: FRAP of EGFP-tagged γ-actin mutants. Cells were scanned 10 times, without any interval between scans, to obtain the pre-bleach image/value. The 10^{th} scan in each case is shown here as the pre-bleach image. An area of the microvilli (blue box) was bleached for 3 seconds at 70% laser intensity. The cells were allowed to recover and images were taken every 30 seconds. The image after 4.5' of recovery is shown for each mutant.

T89I: **2-9C**, K118M: **2- 9D**, P264L: **2-9E**, P332A: **2-9F**, T278I: **2-9G**, V370A: **2-9H**

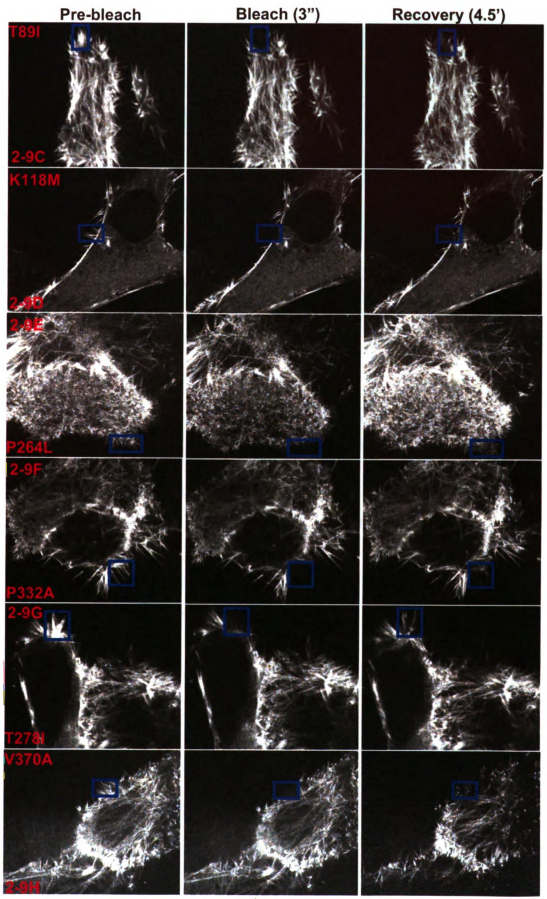
Pre-bleach
Bleach (3")
Recovery (4.5')
T89I
2-9C
K118M
2-9D
2-9E
P264L
2-9F
P332A
2-9G
T278N
V370A
2-9H

Figure 2-10A-10F: Recovery graphs of γ-actin mutants following FRAP. Live cells co-expressing EGFP-γ-actins constructs along with untagged espin were imaged under Olympus Fluoview Fv1000 confocal microscope, for FRAP assay. The pre bleached, bleached and recovered images for each case were analyzed using Metamorph imaging software and the corresponding fluorescent units were further analyzed using KaleidaGraph software to obtain mobile fractions. Time Vs recovery rates for each of the mutants was plotted and compared to the WT recovery. **2-10A**: T89I (n=8) and WT (n=15), **2-10B**: K118M (n=7) and WT, **2-10C**: P264L (n=4) and WT, **2-10D**: P332A (n=9) and WT, **2-10E**: T278I (n=8) and WT, **2-10F**: V370A (n=6) and WT

There was no statistical difference in the recovery rates of mutants and WT γ-actin.

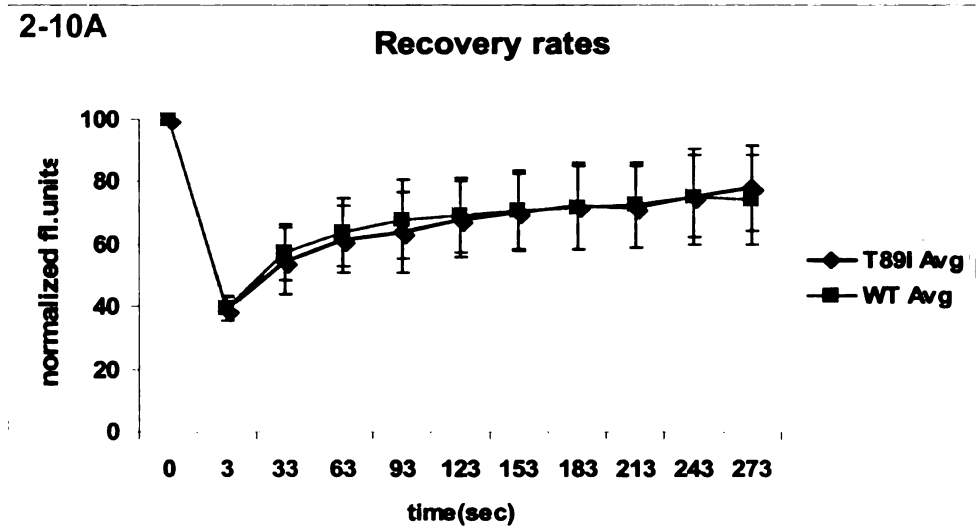
2-10A
Recovery rates
normalized fl.units
100
80
60
40
20
0
0
3
33
63
93
123
153
183
213
243
273
time(sec)
T89I Avg
WT Avg

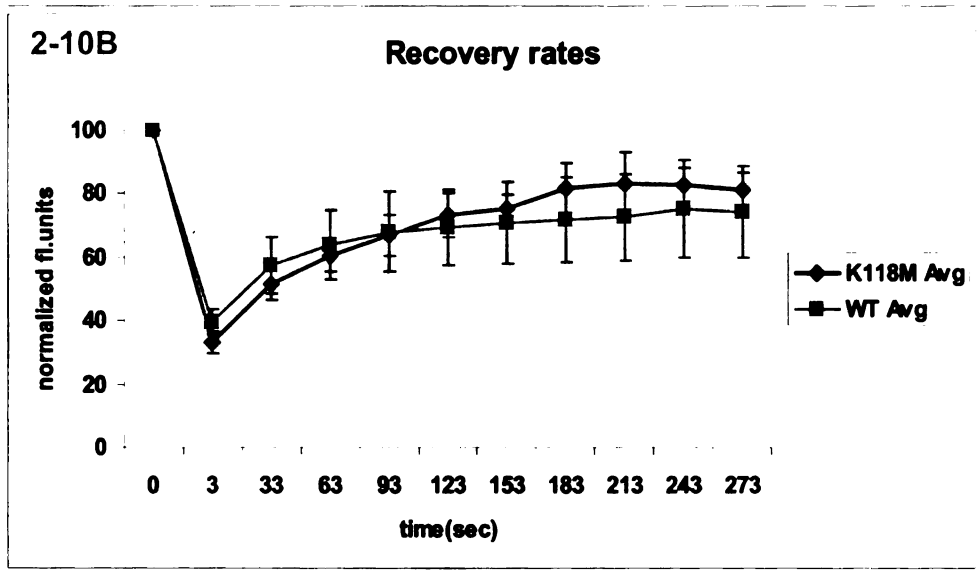
2-10B
Recovery rates
normalized fl.units
100
80
60
40
20
0
0
3
33
63
93
123
153
183
213
243
273
time(sec)
K118M Avg
WT Avg

Figure 2-10A-10F contd

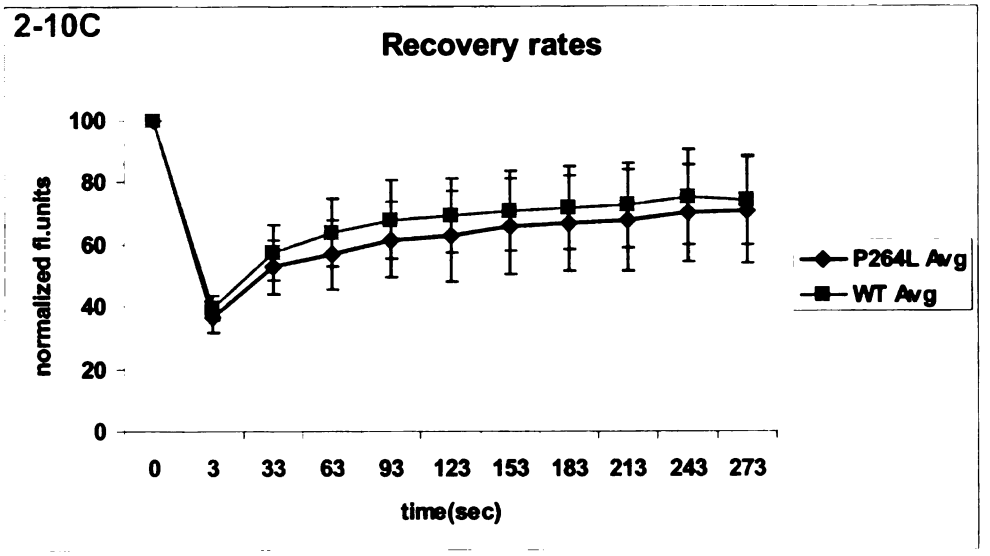

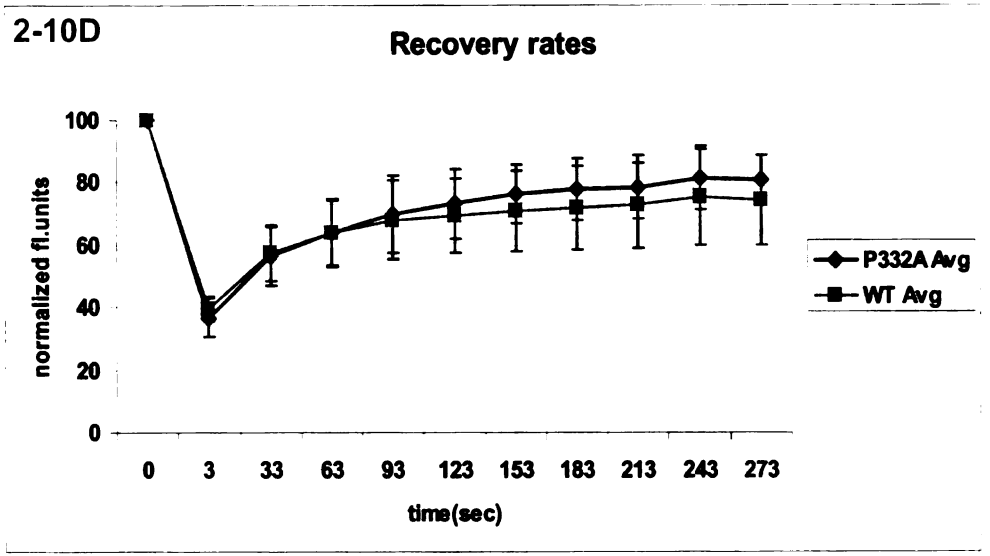

Figure 2-10A-10F contd

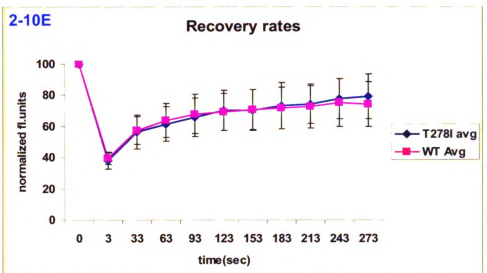

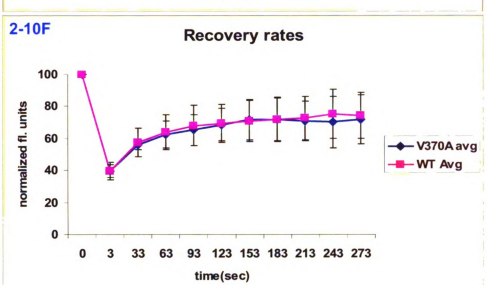

To further confirm that the recovery rates data obtained is indeed an indication of WT and mutant γ-actins mobility and not of EGFP protein, I tried performing FRAP on EGFP alone construct. Following bleach, I expected to see faster recovery rates of the EGFP alone construct, when compared to the EGFP-WTγ-actin. However the EGFP alone construct did not co-localize with espin in the microvilli (Figure 2-11). Hence it was not possible to perform FRAP. This experiment nevertheless confirms the specificity of WT and mutant γ-actins mobility. Current data suggest that the mutant actins, when compared to the WT-actin, do not exhibit differences in cellular mobility.

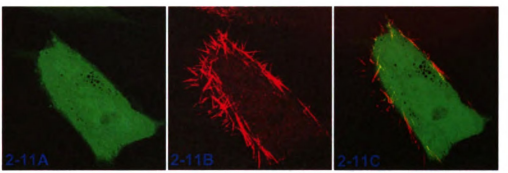

Figure 2-11: Expression of EGFP and DsRed-espin in CL4 cells. DsRed-espin and EGFP-alone constructs were co-transfected in CL4 cells. Cells were imaged under Olympus 1500 confocal microscope, 60X PlanApo objective. **2-11A**: EGFP alone, **2-11B**: DsRed-espin, **2-11C**: Merge. EGFP and espin did not co-localize in the espin. Bar: 10μm

Discussion

Mutations in cytoplasmic γ-actin are shown to cause late-onset, non-syndromic, hearing loss [5, 6, 8]. A ubiquitously expressed and highly conserved protein, γ-actin is the predominant cytoplasmic actin isoform in the inner ear [4]. Recent evidence suggests that γ-actin is not required for the development of the ear, but is essential for the maintenance of actin rich structures [20].

The aim of this dissertation was to determine the functional significance of the initially identified γ-actin missense mutations (T89I, K118M, P264L, P332A, T278I and V370A), which all result in autosomal dominant sensorineural deafness. Since there were no animal models of these mutations, I took a cell-culture approach to evaluate their function.

LLC-PK1-CL4 cells (CL4), porcine proximal kidney epithelial cells, were used to over-express these actin mutations to study the distribution and localization of the mutant actins. Immunohistochemistry of the endogenous actins showed spatial differences in the distribution of cytoplasmic actin isoforms. A functional diversity among the cytoplasmic actins has long been suggested, and shown in many cells types [1]. My data from actively proliferating CL4 cells suggest that β-actin is found in the leading edge of the cells and in stress fibers while γ-actin is found mostly in the cytoplasm and stress fibers. In confluent cells, both β and γ-actins were observed in the periphery and perinuclear space. γ-Actin stained strongly in the cytoplasm compared to β-actin.

All the six γ-actin mutants when over-expressed as N-terminal tagged EGFP constructs localized to key actin rich structures in cells. Over-expression did not result in any morphological changes and the cells were healthy like their WT control.

Espin, an actin-bundling protein, is highly expressed in the stereocilia of the hair cells [12]. It bundles filamentous actin in stereocilia to give them a paracrystalline structure, which is essential for their functioning [19]. CL4 epithelial cells do not express espin endogenously but form long, spiky microvilli when espin is exogenously expressed. Stereocilia are microvilli based mechanotranducers and share many structural and functional similarities; therefore we chose to examine the effect of γ-actin mutations in these structures. Initial studies demonstrated that all the six mutants when co-expressed with espin localized with espin in the microvilli.

On careful observation and measurements, it was determined that the lengths of microvilli expressing the mutant γ-actins were ~20-25% shorter than the WT counterparts. This is an interesting and exciting finding because mutations in proteins like espin, myosin XVa and whirlin have been shown to cause shortening of stereocilia resulting in hearing loss [14, 25, 28, 29]. This result was also quite unexpected since we were predicting to see a phenotype specific to only two of the six mutations, those located in the actin-bundling domain (T89I, K118M). Thus this data suggest that all the six γ-actin mutants

might not be functioning via the same molecular mechanism yet end up resulting in the same phenotype.

I performed cytochalasin D treatments on the microvilli to determine if mutant γ-actins were defective in the repair of damaged structures. Under the conditions used in these experiments, I did not observe any difference in the repair properties of the mutant actins. These data suggest that mutant γ-actins are functioning possibly by dominant negative or gain of function phenomenons, thereby interfering with WT γ-actin filament dynamics.

In an attempt to evaluate the molecular basis of shorter microvilli, I performed fluorescence recovery after photobleaching (FRAP) assays. I hypothesized that the mutant actins would show defects in recovery, when compared to WT γ-actin control, thus suggesting altered mobility or filament incorporation of γ-actin mutant proteins. Results from this assay suggest that the six mutant actins display similar recovery rates and are not significantly different from the WT γ-actin. FRAP was previously performed in CL4 cells to determine the recovery rates of WT β-actin [19] in the microvilli. Data from this dissertation suggest no difference in the recovery rates of WT γ-actin and β-actin.

Recent data from biochemical assays from the Rubenstein lab show that the six mutant γ-actins show varied levels of binding-affinity to cofilin [27]. In-vitro binding assays performed by a previous graduate student in our lab showed that

three mutants exhibited weaker binding with the actin-binding protein CAP (unpublished data). Humans carrying γ-actin mutations do not exhibit hearing loss till the 2nd decade [5]. These mutations hence result in a mild phenotype, a phenomenon also observed in this dissertation in the expression studies and FRAP assays, along with protein binding assays (as performed by Mei Zhu, a previous graduate student). Studying the molecular function of mutant proteins causing a late onset disease can be complicated, even more so when the mutant proteins result in a mild phenotype.

Persons harboring γ-actin mutations display only hearing loss as a phenotype [5, 6, 30]. The inner ear is a complex and specialized tissue. γ-Actin, the predominant isoform is believed to play a critical non-overlapping role in hair cells. Recent data indicate that γ-actin is essential for repair of damaged stereocilia and that β-actin cannot perform this function [20]. In other cell types where β-actin is the predominant isoform, it is possible it performs major cellular functions and overlaps in function with γ-actin. Thus, mutations in γ-actin might not cause any other phenotype except hearing loss.

Data from the first part of this dissertation show that cell culture studies can be a valuable tool in performing functional studies on mutant proteins known to cause hearing loss. The cell culture model provides the flexibility to not only study expression and localization of proteins but also to determine functional aspects like protein mobility *in vivo*.

REFERENCES

1. Khaitlina, S.Y., *Functional specificity of actin isoforms*, in *International Review of Cytology - a Survey of Cell Biology, Vol. 202*. 2001. p. 35-98.

2. Rubenstein, P.A. and K.K. Wen, *Lights, camera, actin.* Iubmb Life, 2005. **57**(10): p. 683-687.

3. Furness, D.N., et al., *Differential distribution of beta- and gamma-actin in guinea-pig cochlear sensory and supporting cells.* Hearing Research, 2005. **207**(1-2): p. 22-34.

4. Hofer, D., W. Ness, and D. Drenckhahn, *Sorting of actin isoforms in chicken auditory hair cells.* Journal of Cell Science, 1997. **110**: p. 765-770.

5. Zhu, M., et al., *Mutations in the gamma-actin gene (ACTG1) are associated with dominant progressive deafness (DFNA20/26).* American Journal of Human Genetics, 2003. **73**(5): p. 1082-1091.

6. van Wijk, E., et al., *A mutation in the gamma actin 1 (ACTG1) gene causes autosomal dominant hearing loss (DFNA20/26).* Journal of Medical Genetics, 2003. **40**(12): p. 879-884.

7. de Heer, A.M.R., et al., *Audiometric and Vestibular Features in a Second Dutch DFNA20/26 Family With a Novel Mutation in ACTG1.* Annals Of Otology Rhinology And Laryngology, 2009. **118**(5): p. 382-390.

8. Liu, P., et al., *Novel ACTG1 mutation causing autosomal dominant non-syndromic hearing impairment in a Chinese family.* Journal Of Genetics And Genomics, 2008. **35**(9): p. 553-558.

9. Drenckhahn, D., et al., *3 Different Actin Filament Assemblies Occur in Every Hair Cell - Each Contains a Specific Actin Cross-Linking Protein.* Journal of Cell Biology, 1991. **112**(4): p. 641-651.

10. Tilney, L.G., M.S. Tilney, and D.J. Derosier, *Actin-Filaments, Stereocilia, and Hair-Cells - How Cells Count and Measure.* Annual Review of Cell Biology, 1992. **8**: p. 257-274.

11. Bartles, J.R., et al., *Espin is the missing crosslinker in the actin bundles of hair cell stereocilia.* Molecular Biology of the Cell, 1998. **9**: p. 135A-135A.

12. Sekerkova, G., et al., *Espins are multifunctional actin cytoskeletal regulatory proteins in the microvilli of chemosensory and mechanosensory cells.* Journal of Neuroscience, 2004. **24**(23): p. 5445-5456.

13. Li, H.W., et al., *Correlation of expression of the actin filament-bundling protein espin with stereociliary bundle formation in the developing inner ear.* Journal of Comparative Neurology, 2004. **468**(1): p. 125-134.

14. Zheng, L.L., et al., *The deaf jerker mouse has a mutation in the gene encoding the espin actin-bundling proteins of hair cell stereocilia and lacks espins.* Cell, 2000. **102**(3): p. 377-385.

15. Tyska, M.J. and M.S. Mooseker, *MYO1A (brush border myosin I) dynamics in the brush border of LLC-PK1-CL4 cells.* Biophysical Journal, 2002. **82**(4): p. 1869-1883.

16. Bryan, K.E., et al., *Effects of human deafness gamma-actin mutations (DFNA20/26) on actin function.* Journal Of Biological Chemistry, 2006. **281**(29): p. 20129-20139.

17. Otey, C.A., et al., *Immunolocalization of the Gamma-Isoform of Nonmuscle Actin in Cultured-Cells.* Journal of Cell Biology, 1986. **102**(5): p. 1726-1737.

18. Hill, M.A. and P. Gunning, *Beta-Actin and Gamma-Actin Messenger-Rnas Are Differentially Located within Myoblasts.* Journal of Cell Biology, 1993. **122**(4): p. 825-832.

19. Loomis, P.A., et al., *Espin cross-links cause the elongation of microvillus-type parallel actin bundles in vivo.* Journal of Cell Biology, 2003. **163**(5): p. 1045-1055.

20. Belyantseva, I.A., et al., *gamma-Actin is required for cytoskeletal maintenance but not development.* Proceedings Of The National Academy Of Sciences Of The United States Of America, 2009. **106**(24): p. 9703-9708.

21. Pollard, T.D. and G.G. Borisy, *Cellular motility driven by assembly and disassembly of actin filaments (vol 112, pg 453, 2002).* Cell, 2003. **113**(4): p. 549-549.

22. Belyantseva, I.A., et al., *Stereocilia: the long and the short of it.* Trends in Molecular Medicine, 2003. **9**(11): p. 458-461.

23. Rzadzinska, A.K., et al., *An actin molecular treadmill and myosins maintain stereocilia functional architecture and self-renewal.* Journal of Cell Biology, 2004. **164**(6): p. 887-897.

24. Rommelaere, H., et al., *Structural plasticity of functional actin: Pictures of actin binding protein and polymer interfaces.* Structure, 2003. **11**(10): p. 1279-1289.

25. Belyantseva, I.A., et al., *Myosin-XVa is required for tip localization of whirlin and differential elongation of hair-cell stereocilia.* Nature Cell Biology, 2005. **7**(2): p. 148-U60.

26. Donaudy, F., et al., *Espin gene (ESPN) mutations associated with autosomal dominant hearing loss cause defects in microvillar elongation or organisation.* Journal of Medical Genetics, 2006. **43**(2): p. 157-161.

27. Bryan, K.E. and P.A. Rubenstein, *Allele-specific Effects of Human Deafness gamma-Actin Mutations (DFNA20/26) on the Actin/Cofilin Interaction.* Journal Of Biological Chemistry, 2009. **284**(27): p. 18260-18269.

28. Mburu, P., et al., *Defects in whirlin, a PDZ domain molecule involved in stereocilia elongation, cause deafness in the whirler mouse and families with DFNB31.* Nature Genetics, 2003. **34**(4): p. 421-428.

29. Kikkawa, Y., et al., *Mutant analysis reveals whirlin as a dynamic organizer in the growing hair cell stereocilium.* Human Molecular Genetics, 2005. **14**(3): p. 391-400.

30. Rendtorff, N.D., et al., *A novel missense mutation in ACTG1 causes dominant deafness in a Norwegian DFNA20/26 family, but ACTG1 mutations are not frequent among families with hereditary hearing*

impairment. European Journal Of Human Genetics, 2006. **14**(10): p. 1097-1105.

32. Snapp,EL., Altan N., et al., *Measuring protein mobility by photobleaching GFP chimeras in living cells. Current Protocols in Cell Biology,2003,21.1-21.1.24*

CHAPTER 3

Transgenic zebrafish model of γ-actin mutations

Abstract

Using a multi-site Gateway system, EGFP tagged WT and mutant γ-actin constructs were made to create a transgenic zebrafish model for the γ-actin mutants. These constructs, under a heat shock promoter, were used to over-express the mutant actins in the zebrafish. Confocal images of hair cells of cristae and maculae from fish at 4-day post fertilization (dpf) showed that five out of six mutants are expressed in hair cells and stereocilia. Fish harboring these mutations did not show any morphological defects and appeared healthy like the WT counterparts.

Introduction

Zebrafish inner ear architecture

Zebrafish, *Danio rerio*, has an ear organization similar to other vertebrates. Since it has a rapid development and the embryo is transparent, it is an excellent model system to visualize inner ear development in vivo and in whole mounts [1, 2].

The inner ear of zebrafish consists of utricle, saccule and lagena, the three communicating chambers and three semicircular canals that open into the utricle (Figure 3-1). The chambers and the canals house the sensory epithelium. Each patch of sensory epithelium consists of hair cells and supporting cells associated with sensory neurons to relay signals to the brain. The various sensory patches however perform different mechanosensory roles. The patches associated with the semicircular canals are known as cristae, act as sensors of rotational acceleration. The patches of the utricle, saccule and lagena, known as maculae, detect linear acceleration, gravity and sound [1, 2]. A crystalline deposit of calcium carbonate known as otolith overlies each macula, which facilitates its function. The characteristic features of all the hair cells are a single tubulin based kinocilium and the actin filled stereociliary bundles, which are the mechanotransducers of sound.

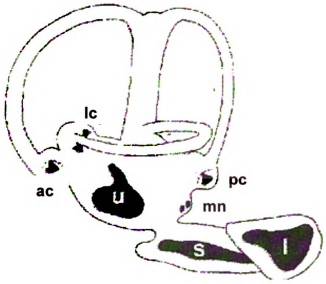

Figure 3-1: Sketch of an adult zebrafish ear ([1]. The sensory patches are in black. Three cristae: anterior (ac), posterior (pc) and lateral (lc). Three maculae: utricle (u), saccule (s) and lagena (l) and a pair of small patches: macula neglecta (mn).

Zebrafish inner ear development

The zebrafish inner ear forms on either side of the hindbrain in the developing fish. The ear originates from the ectodermal thickening, otic placode ,which over time invaginates to form the otic vesicle [2]. All the inner ear structures develop from the otic vesicle.

At ~24 hrs post fertilization (hpf), the first sensory patches on the macula are observed. By 42 hpf, 10-20 hair cells in each macula are observed, with the number increasing to ~80 by 72 hpf. The semicircular canals and their sensory patches, the cristae, differentiate much later, between 42-72 hpf [1]. Since all the sensory epithelia of the inner ear differentiate completely by 72 hpf, and the fish have functional ears by 96 hpf, fish in this stage prove to be a good model to study protein expression/localization in the sensory epithelium [3].

Transgenic model overview

As previously described by Kwan *et al*, a Tol2 based multi-site Gateway system was used to clone GFP tagged-human WT and the six mutant γ-actins [4] for over-expression in zebrafish. This transposase, site-specific recombination based technique has the advantages of allowing one to quickly build complex constructs with high efficiency. The details of the constructs are provided in the 'results' section.

The actin constructs, under a heat shock promoter, were injected into zebrafish embryos, which were heat shocked to over-express the actins. Ears of fish at 4 days post fertilization (dpf) fish were imaged with a Zeiss confocal microscope. Five mutant actins localize to the sensory epithelium and the stereocilia. No morphological changes/defects were observed in the fish harboring these mutations.

These data are consistent with the cell culture localization results, in which the mutant actins localized to actin-rich structures like the microvilli. The data also suggest that in the zebrafish, γ-actin mutants do not cause developmental defects in the ear, which is consistent with the human phenotype [5]. This is also consistent with recently published data on a γ-actin KO mouse model, where it was shown that γ-actin is not required for embryogenesis [6].

Materials and Methods

Zebrafish lines and handling: WT fish were used. Adult fish and embryos were raised at 28.5°C.

Plasmid Construction: The 5' and 3' entry clones (carrying 5' promoter and IRES-EGFP respectively) and destination vector (pDestTol2pA2) were a kind gift from Dr. Jarema Malicki's lab at MEEI, Boston MA. PCR based assay was used to construct the middle entry clone carrying EGFP-actin inserts (details in Results section).

RNA Synthesis: Transposase RNA was generated using the pCS2FA-transposase plasmid as a template. DNA was linearized with *Not*I and purified using the Qiagen PCR Purification Kit. Capped RNA synthesis was performed using the mMessage mMachine SP6 kit (Ambion). RNA was purified using the Qiagen RNeasy Mini Kit.

Injections: Expression constructs were tested by injection of plasmid DNA, with transposase RNA, into the cell at the one-cell embryo. 25 or 30 pg of DNA was injected with 25 pg of transposase RNA. ~200 embryos were injected out of which ~ 20 were imaged.

Heat Shock: Embryos were incubated in E3 embryo medium pre warmed to 37°C and heat-shocked for 45 min at 37°C.

Imaging: Confocal imaging was performed on a Zeiss scope. Embryos were mounted in 1.0% low melting point agarose. Images were captured using a 60X-dipping lens.

Results

The cell culture model has been very informative in delineating the functional significance of human γ-actin mutations (Chapter 2). However, these mutations have not been experimentally expressed in any complex model organism thus far. To this end, we set out to over-express these mutations in the zebrafish, an organism widely used to study genes involved in human diseases. The rationale behind over-expressing these mutants in zebrafish was to determine the localization of the mutant actins in the ear. We also hoped to measure the lengths of stereocilia and based on our cell culture observations, we expected them to be shorter compared to the WT controls.

Vector Construction

A multi-site Gateway based approach was used to generate the expression constructs. Gateway cloning technology uses *att* site-specific recombination system from lambda phage [7]. In the multi-site approach, various *att* sites can be used to directionally combine ~ five fragments of DNA (entry clones). The Tol2 kit, which uses the Tol2 transposon backbone, is designed to make expression constructs which robustly over-express in zebrafish [4]. To over-express the human γ-actin mutations in zebrafish, a multi-site Gateway based Tol2 kit was used. Here, 3 entry clones were combined into a 'destination' vector. pDestTol2pA2, the destination vector contains *attR4-attR3* site, with SV40 polyA, flanked byTol2 inverted repeats (Figure 3-2A).

The 3 entry clones are referred to as 5pE, 3pE and ME. The 5' element, 5pE, typically consists of a promoter element, which is flanked by *attL4-attR1* sites. The 3' element, 3pE contains a poly A signal or a 3' tag such as IRES-poly A, flanked by *attR2-attL3* sites. The middle element or ME contains a reporter or coding sequence of the gene of interest, flanked by *attL1-attL2* (Figure 3-2A). The entry clones are generated using PCR to add *attB* sites to the ends of desired inserts, and recombined using a BP recombinase into pDONR221 vector (where *attB-attP* sites recombine) and transformed into bacteria.

The 5' entry clone, containing 1.5kb of hsp70 (heat shock promoter), 3pE, containing IRES (internal ribosome entry site) driving expression of EGFP-polyA, and the pDestTol2pA2 vectors were a kind gift from Jarema Malicki at Massachusetts Eye and Ear Infirmary (MEEI). I generated the ME entry clone by PCR to add *attB* sites to the ends of EGFP- γ-actin (WT or mutant) followed by a BP reaction to recombine into pDONR221 vector (Figure 3-2B). EGFP fusion constructs were used to facilitate visualization of actin localization, and because similar fusion constructs were used previously in cell culture studies (Materials and Methods-Chapter 2).

To generate the final expression construct, equimolar amounts of all the three entry clones: 5pE, 3pE, ME and destination vector were mixed *invitro* in a LR reaction (where the *attL-attR* sites recombine) and transformed in bacteria

Figure 3-2: Multi-site gateway-based construction of expression vectors (modified from [4]. 3-2A: Schematic representation of pDestTol2pA2, 5' entry clone, 3' entry clone and middle element vector backbones. pDestTol2pA2 empty vector contains a ccdB/cmR (chloremphenicol) cassette, which is flanked by *attR4* and *attR*3 sites. p5E contains *attL4* and att *R1*, p3E contains *attR2* and *attL3*, while the middle element contains *attL1* and *attL2* sites. **3-2B**: *att* sites are added to the entry clones by PCR. An example of adding *att* sites to middle element (EGFP-actin) is illustrated here. A 'BP' reaction is performed to recombine the PCR product into an entry vector like pDONR221. This results in EGFP-actin fusion insert flanked by *attL1* and *attL2*. **3-2C**: A 'LR' reaction is performed where equimolar amounts of p5E, 3pE, ME and pDestTol2pA2 vectors are recombined together to get the final expression construct. **3-2D**: In spite of being *att* site-specific recombination reaction, fragments do recombine in wrong orientations [4]. A diagnostic restriction digestion was designed and performed to confirm the correct orientation of the fragments. Correctly recombined fragments give two fragments of 3.3kb and 5.99kb when digested with EcoRI. **3-2E**: Constructs that gave the correct digestion pattern were sequenced to confirm the sequence of *att* sites. 5 different primers were designed to cover all the *att* sites (Appendix-I).

3-2A

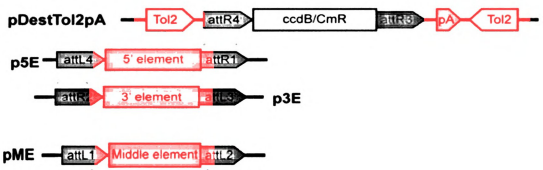
pDestTol2pA
Tol2
attR4
ccdB/CmR
attR3
pA
Tol2
p5E
attL4
5' element
attR1
attR2
3' element
attL3
p3E
pME
attL1
Middle element
attL2

3-2B

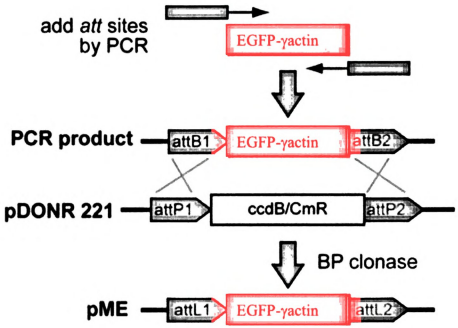
add att sites
by PCR
EGFP-γactin
PCR product
attB1
EGFP-γactin
attB2
pDONR 221
attP1
ccdB/CmR
attP2
BP clonase
pME
attL1
EGFP-γactin
attL2

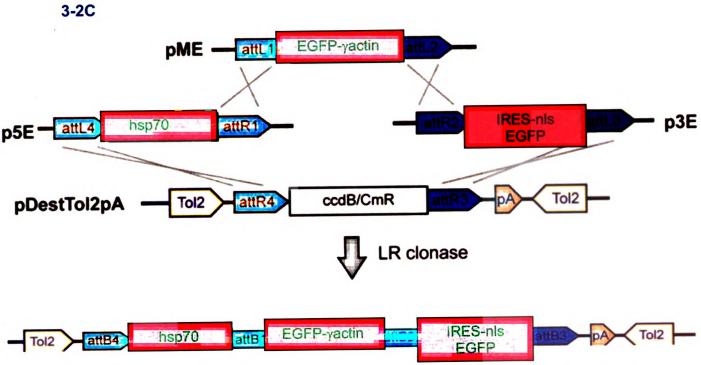
3-2C
pME
attL1
EGFP-γactin
attL2
p5E
attL4
hsp70
attR1
attR3
IRES-nls
EGFP
p3E
pDestTol2pA
Tol2
attR4
ccdB/CmR
attR3
pA
Tol2
LR clonase
Tol2
attB4
hsp70
attB
EGFP-γactin
IRES-nls
EGFP
attB3
pA
Tol2

3-2D

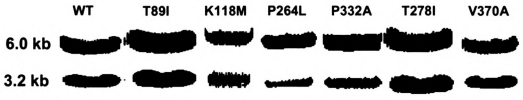
WT
T89I
K118M
P264L
P332A
T278I
V370A
6.0 kb
3.2 kb

3-2E


pDestTol2pA2 5' thru attR4 shared (1-1100bp)
Primer-1, 5' attR4
hsp70 insert (1100-2680bp)
Primer 3, attR1
EGFP-actin (2690-4590bp)
Primer 4, attR2
IRES-nls EGFP (4580-6193bp)
pDestTol2pA2 3' thru attR3 shared (6203-9238bp)
Primer 5, 3' attR3

with antibiotic selection (Figure 3-2C). The orientation of the constructs was confirmed by restriction digestion and sequencing (Figure 3-2E).

Expression of human γ-actin mutants in the zebrafish ear

The expression studies were conducted in the Malicki lab at MEEI over a period of 3 1/2 weeks. To enhance the rate of plasmid integration and expression levels, plasmid DNA was injected along with transposase RNA into one-cell embryos on day 0. To induce the expression of the EGFP-tagged actins, the embryos were heat-shocked at 37°C for 45 minutes on day 1. Robust EGFP expression was observed in the fish embryo within 2 hours of induction (Figure 3-3). The fish were heat-shocked again on day 3 to enhance the EGFP expression. On day 4, fish were fixed and immunostained for acetylated-α-tubulin. This protein is specific for ciliary structures [8], and hence was helpful in locating the ear structures under the confocal microscope. In addition, measuring the lengths of the cilia would have been pivotal in determining the lengths of the stereocilia (determining the ratios of cilia: stereocilia would be an accurate measure of the stereocilia lengths).

Expression of the γ-actins in the cristae of zebrafish ear

Cristae, the sensory patches associated with semi-circular canals allow for localization under a confocal microscope. Hence I imaged the crista (mostly anterior) to determine the localization of the human WT and mutant γ-actins and

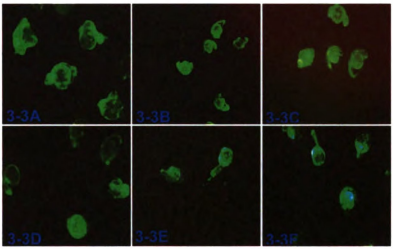

Figure 3-3: EGFP expression in the zebrafish embryo following heat-shock. EGFP-actin constructs were injected into 1 cell embryo and heat shocked after 24 hrs for 45 min at 37°C. EGFP expression was observed within 2 hrs of heat shock. **3-3A**: EGFP-WT, **3-3B**: EGFP-T89I, **3-3C**: EGFP-K118M, **3-3D**: EGFP-P264L, **3-3E**:EGFP-P332A, **3-3F**: EGFP-T278I

to examine the stereociliary structures of mutant actin expressing cells. Human actins localized to the hair cells and the stereocilia of the anterior crista (Figure 3-4). As seen in Figure 3-4, WT and the mutant actins were expressed and localized to the sensory epithelium of the anterior crista. However, I was unable to get a successful expression of EGFP-T278I mutant γ-actin in the 4dpf zebrafish embryo. The possible reasons will be discussed in the Discussion section.

Expression of the γ-actins in the maculae of zebrafish ear

In addition to the cristae, I imaged the macula of the fish ears to determine if the mutant actins localized to all the sensory epithelia of the ear. As expected, WT and all mutant γ-actins (except EGFP-T278I) localized to the hair cells and the stereocilia of the macula (Figure 3-5). I did not observe any difference in the expression levels or localizations of WT and mutant actins between the sensory epithelia of crista and macula.

Stereocilia lengths determination

It was not possible to determine the lengths of the stereocilia. Accurate measurements would require further standardization of transgene expression. Scanning electron microscopy (SEM) could be a better technique to measure stereociliary lengths because the stereocilia of the zebrafish ear are too small for accurate measurements using confocal studies. In addition, individual

Figure 3-4: Expression of γ-actin mutants in the crista of zebrafish ear. pDest Tol2pA2 expression vectors carrying EGFP-actin fusion inserts and Transposase RNA were injected into1-cell embryos. The fish were heat-shocked and 4dpf fish were fixed and immunostained for acetylated-α-tubulin (secondary antibody tagged with AlexaFluor 546) and imaged under a 100X dipping lense of Zeiss confocal microscope. Cilia are seen in red. **3-4A**: Anterior crista showing expression of EGFP-WT actin in the hair cells and stereocilia. Bar: 12.5μm. **3-4B**: Anterior crista showing expression of EGFP-T89I actin in the hair cells and stereocilia. Bar: 25μm. **3C**: Anterior crista showing expression of EGFP-K118M actin in the hair cells and stereocilia. Bar: 25μm. **3-4D**: Anterior crista showing expression of EGFP-P332A actin in the hair cells and stereocilia. Bar: 15μm. **3-4E**: Anterior crista showing expression of EGFP-V370A actin in the hair cells and stereocilia. Bar: 25μm.

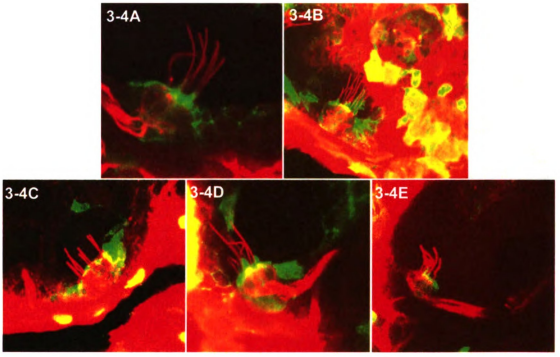
3-4A
3-4B
3-4C
3-4D
3-4E

Figure 3-5: Expression of γ-actin mutants in the macula of zebrafish ear. pDest Tol2pA2 expression vectors carrying EGFP-actin fusion inserts and Transposase RNA were injected into1-cell embryos. The fish were heat-shocked and 4dpf fish were fixed and immunostained for acetylated-α-tubulin (secondary antibody tagged with AlexaFluor 546) and imaged under a100X dipping lense of Zeiss confocal microscope. Cilia are seen in red. **3-5A**: Macula showing expression of EGFP-WT actin in the hair cells and stereocilia. Bar: 25μm. **3-5B**: Macula showing expression of EGFP-T89I actin in the hair cells and stereocilia. Bar: 25μm. **3-5C**: Macula showing expression of EGFP-K118M actin in the hair cells and stereocilia. Bar: 25μm. **3-5D**: Macula showing expression of EGFP-P264L actin in the hair cells and stereocilia. Bar: 25μm. **3-5E**: Macula showing expression of EGFP-P332A actin in the hair cells and stereocilia. Bar: 25μm.

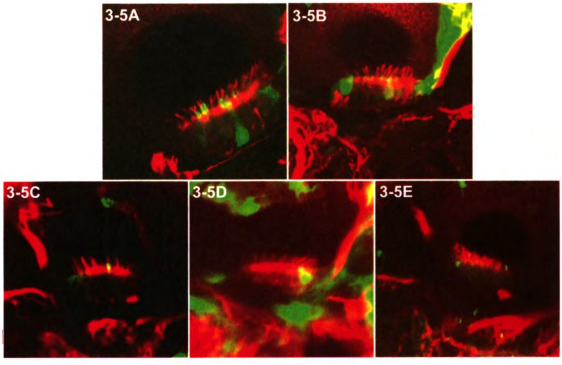
3-5A
3-5B
3-5C
3-5D
3-5E

Stereocilium measurement would require a technique like SEM. Considering the restrain on resources and time, I was not able to pursue stereocilia length measurement assays further.

Discussion and future directions

I designed multi-site Gateway based expression constructs to generate transgenic zebrafish expressing mutant γ-actin. Based on the uniquely designed Tol2kit transposon backbone, I was able to express, for the first time, human WT and mutant γ-actins in an intact animal model, the zebrafish. As part of the expression studies, I was able to determine that the mutant actins (except one), which cause non-syndromic hearing loss in human populations, can be expressed in the sensory epithelia of zebrafish ear. Over-expression did not result in any obvious morphological changes/defects in the young fish as a whole or in the ears. The mutant fish ears were indistinguishable from their WT counter parts (data not shown).

I was unable to generate a transgenic zebrafish expressing EGFP-T278I mutant. In one attempt, while other regions of the fish were fluorescent, GFP expression was not detected in the ears of the fish. In another attempt, I did not observe any GFP expression in 1dpf fish following heat-shock induction. There is no reason to believe that this mutant should behave any differently than the other mutants (in cell culture studies, T278I did not show any marked difference compared to the other mutants). Hence, more attempts at injecting this mutant into the zebrafish embryos will be required to determine its expression and localization.

To determine if expression of the mutants results in shortening of the stereocilia, further standardization is required. Different constructs show different expression levels (Figure 3-4,3-5), which in turn seem to determine if protein expression is seen in stereocilia. Determining the minimum level of expression required for localization in hair cells and stereocilia will be informative for future experiments. Additionally, scanning electron microscopy of the stereocilia will be ideal for measuring individual stereocilium lengths.

One alternative to overcoming the above-mentioned caveats is to perform expression studies in transgenic lines of these mutants. Germ line transmission of genes is relatively low in zebrafish [4], but using robust integration techniques like the Tol2 kit, higher rates of germ line transmission can be achieved.

APPENDIX-1

Primer sequences to sequence *att* sites in pDestTol2pA2 expression construct

Primer 1: Forward primer: CACCAGAAATGCCCTCTGAT (412 from start of vector, 5' of hsp 70)

Primer 2: Reverse primer: CCTCCTTGTTCAGTCGTGGT (300 from start site of hsp70)

Primer 3: Forward primer: GAGCAGCCTGACAGGACTTT (1007 from start site of hsp70)

Primer 4:Reverse primer: AGGCTACAGCTTCACCACCA (in γ-actin)

Primer 5: Reverse primer: GCTATGTGGCGCGGTATTAT (343 away from end;3' of IRES-nls EGFP)

REFERENCES

1. Haddon, C. and J. Lewis, *Early ear development in the embryo of the zebrafish, Danio rerio.* Journal Of Comparative Neurology, 1996. **365**(1): p. 113-128.

2. Whitfield, T.T., et al., *Development of the zebrafish inner ear.* Developmental Dynamics, 2002. **223**(4): p. 427-458.

3. Nicolson, T., *The genetics of hearing and balance in zebrafish.* Annual Review Of Genetics, 2005. **39**: p. 9-22.

4. Kwan, K.M., et al., *The Tol2kit: A multisite Gateway-based construction kit for Tol2 transposon transgenesis constructs.* Developmental Dynamics, 2007. **236**(11): p. 3088-3099.

5. Zhu, M., et al., *Mutations in the gamma-actin gene (ACTG1) are associated with dominant progressive deafness (DFNA20/26).* American Journal of Human Genetics, 2003. **73**(5): p. 1082-1091.

6. Belyantseva, I.A., et al., *gamma-Actin is required for cytoskeletal maintenance but not development.* Proceedings Of The National Academy Of Sciences Of The United States Of America, 2009. **106**(24): p. 9703-9708.

7. Hartley, J.L., G.F. Temple, and M.A. Brasch, *DNA cloning using in vitro site-specific recombination.* Genome Research, 2000. **10**(11): p. 1788-1795.

8. Tsujikawa, M. and J. Malicki, *Intraflagellar transport genes are essential for differentiation and survival of vertebrate sensory neurons.* Neuron, 2004. **42**(5): p. 703-716.

CHAPTER 4

Summary, Discussion & Future Directions

In this dissertation, I have attempted to dissect the molecular functions of six cytoplasmic γ-actin mutations (T89I, K118M, P264L, P332A, T278I and V370A) that cause autosomal dominant, non-syndromic, progressive sensorineural hearing loss. Initially identified by our lab and others, these γ-actin mutations cause mild to profound hearing loss in patients. Hearing loss is detected in the 2nd decade in these persons with some variation between families in onset and rates of progression. γ-Actin is the predominant cytoplasmic actin isoform in the inner ear and is found extensively in the stereocilia and other actin rich structures of the hair cell.

Animal models of hearing loss are pivotal in dissecting the patho-physiology of human hearing loss. Since there isn't an animal model for these mutations, I chose to develop a cell culture model for their study. In addition I was able to make a transgenic zebrafish model of these mutations. LLC-PK1-CL4 (CL4) cells, a porcine kidney tubular epithelial cell line, were used to perform expression and cell localization studies. This particular cell line was chosen for many reasons. This cell line is easily transfectable and has been routinely used to study the dynamics of cytoskeletal proteins. More importantly, these cells make long spikey microvilli when transfected with the actin-bundling protein espin. Espin is one of the actin-bundling proteins expressed in the ear while stereocilia, the mechano transducers of the inner ear, are microvilli like projections. Besides the similarities in structure and protein compositions of stereocilia and microvilli, T89I and K18M mutations are in the predicted actin-

bundling domain of the protein, and hypothesized to interfere with actin filament bundling sites. Thus CL4 cells were considered ideal for evaluating these and other mutations.

Over-expression of the six γ-actin mutants in CL4 cells did not induce any detectable phenotype. All the six mutants behaved like the WT control in the distribution and localization patterns. When co-expressed with espin, all the mutants localized with espin in the microvilli, like the WT counterpart. Initially I worked with two mutants, T89I and K118M, since they seemed quite interesting and appropriate to study bundling properties. However, when the lengths of the microvilli were compared, I found that the microvilli expressing the mutants were ~20-25% shorter than the microvilli expressing WT γ-actin. This experiment was repeated at least 3 times to confirm reproducibility. To further confirm this data, microvilli of untransfected cells were measured and there was no difference observed in the lengths between mutant and WT untransfected cells. At this point I measured the lengths of microvilli expressing the rest of the mutants and found that the microvilli lengths were indeed 20-25% of those expressing WT γ-actin. This is a significant finding because for the first time we have a measurable difference in phenotype associated with these mutations. In addition, there is evidence in the literature that suggests shorter/ shortening of stereocilia results in hearing loss. Mutations in proteins like espin and myosin XVa, also expressed in the stereocilia, result in shorter/shortening of stereocilia eventually resulting in hearing loss. Mutant espin protein is believed to form a weak binding partner with

actin, as a result the actin filaments in the stereocilia are not bundled tightly. The stereocilia become shorter and eventually are absorbed into the hair cells. Mutations in Myosin XVa on the other hand result in abnormally short stereocilia and aberrant staircase structure, a phenotype restored when WT myosin XVa is delivered to the mutant stereocilia. It is hypothesized that the interaction of myosin XVa with whirlin, a PDZ domain protein, is essential for the elongation of stereocilia.

Data from a γ-actin knockout mouse model show mice developing hearing loss in higher frequencies around 16 weeks of age. This suggests that γ-actin is not absolutely required for ear embryogenesis. The knockout mice however fail to maintain structural integrity of the stereocilia actin core as evidenced by gaps in the stereociliary bundles of these mice. These data suggest that γ-actin might be essential for the maintenance of actin structures in the ear. To determine if the γ-actin mutations were defective in repair and maintenance of actin filaments, cytochalasin D treatments were performed on the microvilli of cells expressing T89I and K118M (because of the location of these mutations in the bundling domain of actin). There was no detectable difference in the recovery rates of mutant and WT actins, and the recovering mutant microvilli were no longer than the untreated microvilli. Hence there continued to be a 20-25% difference in lengths between the recovering WT and mutant actin microvilli. Since no difference in the recovery rates between T89I, K118M and WT was observed, this assay was not performed on rest of the four mutants.

To further explore possible causes of shorter microvilli, fluorescence recovery after photobleaching (FRAP) assays were performed on the microvilli. We hypothesized to see differences in the recovery rates of WT and mutant actins, which would be interpreted as defects in actin trafficking or filament incorporation in the microvilli. Defects in actin trafficking is an indirect measure of defective binding of actin and actin binding proteins. These experiments however did not reveal any significant differences between the recovery rates of WT and mutants actins.

The γ-actin mutants are thought to display subtle phenotypes in *in-vitro* studies (previous graduate student's unpublished data and unpublished expression data from guinea pig inner ear explant cultures-personal communication with Dr. Belyantseva). To obtain quantitative and qualitative data of such subtle mutations, more stringent experimental conditions need to be employed. For example with FRAP assays, further standardization like controlling for expression levels of the mutant actins, and number of microvilli to be bleached can be performed. In addition, the microvilli chosen for bleach can be more stringently selected. Above-mentioned alternatives also might not uncover mutant phenotype since, besides being a difficult and time consuming assay, FRAP might not be sensitive enough to show a phenotype with these subtle γ-actin mutations.

Cytochalasin D is an actin filament depolymerizing agent that caps barbed ends of growing filaments. Using cytotochalasin D is one way of simulating damage. It is possible that this 'stressor' does not completely represent 'damage' to actin filaments. Another way to study damage and repair process and/or actin trafficking is Latrunculin A drug treatment. It blocks actin filament elongation by sequestering monomeric actin in the cell. If sequester and subsequent release of monomeric actin results in shorter microvilli in cells expressing mutant actins, it could represent delayed trafficking of actin monomers in the cell.

Another alternative approach to determine the molecular function of the mutations would be to perform an siRNA experiment where the endogenous actin levels are knocked down before over-expressing the mutants. In these conditions, where the mutant actins will be the major actin population in the cell phenotypic effects of the mutations might be more apparent. Standardization of the siRNA conditions can prove to be tricky.

I believe we have learnt a great deal about these mutations from the cell culture model. An animal model might be essential to accurately determine the molecular function of these mutants. Meghan Drummond, a graduate student in the lab, is currently analyzing a mouse knock-in model of the P264L mutation. It will be interesting to know if the stereocilia of this mouse are shorter than their WT littermates. Though the persons carrying these mutations do not exhibit any other phenotype, it will be curious to see if the intestines of these mice exhibit

any subtle disease pathology (γ-actin is also the predominant isoform in the intestinal epithelia). The mouse model however has its disadvantages. It is a time consuming experiment, where at least two years are required to evaluate the model. In addition, with a knock-in model, only one mutant can be a studied, as opposed to cell culture or other animal models like the zebrafish.

I had the opportunity to express and study the localization of all these six γ-actin mutants in the zebrafish ear. Using multi-site gateway cloning technology, I made Tol2 based expression constructs to generate a transgenic zebrafish model of the actin mutants. These mutations result in a mild phenotype, as evidenced by the human and cell culture data. Hence we did not expect to see any development defects in the fish. Localization studies showed that five of the six mutants are expressed in the hair cells and stereocilia of ear crista and macula. They did not affect the development of the ear or the animal as a whole. It will be interesting to determine if over-expression of the mutants results in shortening of stereocilia. It will be essential to standardize the expression levels, as distribution and localization within the hair cell seem to be dependent on protein levels. Alternative approaches will be to construct germ lines of fish expressing equal amounts of the mutant proteins and normalize for mutant and WT actin levels. Another attractive approach will be to study the effect of the mutations in aging fish.

The zebrafish transgenic model is one step towards making animal models of γ-actin mutants. From the human data we know that hearing loss is late onset, thus suggesting that these mutations do not affect the development of the ear. Data from cell culture and zebrafish studies reiterate the same as γ-actin mutations do not affect localization or the distribution of mutant protein and they do not affect the development of the fish ear.

γ-Actin mutants however are suspected to affect filament dynamics that are essential for proper maintenance and functioning of hair cells. Biochemical studies performed on purified yeast actin carrying the human mutations and cofilin, and binding assays of actin and actin binding proteins performed by a previous graduate student, suggest that mutant actins display altered affinities for various actin-binding proteins. To maintain functional filament dynamics in the stereocilia, actin must interact with various binding partners like profilin, ADF/cofilin, espin, and fimbrin at different times in different regions of the cell. It is possible to imagine that the γ-actin mutations do not form strong bonds with these binding partners, which eventually results in weak and shorter filaments.